















2-oxoglutarate-dependent dioxygenases drive expansion of steroidal alkaloid structural diversity in the genus *Solanum*

Prashant D. Sonawane^{1,2} , Adam Jozwiak¹ , Ranjit Barbole^{1,3,4} , Sayantan Panda^{1,5} , Bekele Abebie⁶ , Yana Kazachkova¹ , Sachin A. Gharat¹ , Ofir Ramot⁷, Tamar Unger⁸ , Guy Wizler¹ , Sagit Meir¹ , Ilana Rogachev¹ , Adi Doron-Faigenboim⁹, Marina Petreikov⁹, Arthur Schaffer⁹, Ashok P. Giri^{2,3} , Tali Scherf¹⁰  and Asaph Aharoni¹ 

¹Department of Plant and Environmental Sciences, Weizmann Institute of Science, Rehovot 7610001, Israel; ²Department of Natural Products, Max Planck Institute for Chemical Ecology, Jena 07745, Germany; ³Biochemical Sciences Division, CSIR-National Chemical Laboratory, Pune 411008, India; ⁴Academy of Scientific and Innovative Research (AcSIR), Ghaziabad 201002, India; ⁵Gilat Research Center, Agricultural Research Organization (ARO), Rural delivery Negev 85280, Israel; ⁶Department of Plant Pathology and Weed Research, ARO-Volcani Center, Bet Dagan 50250, Israel; ⁷Metabolic Insights Ltd, Ness Ziona 7414001, Israel; ⁸Israel Structural Proteomics Centre, Weizmann Institute of Science, Rehovot 7610001, Israel; ⁹Institute of Plant Sciences, ARO-Volcani Center, Rishon LeZiyyon 7505101, Israel; ¹⁰NMR unit, Department of Chemical Research Support, Weizmann Institute of Science, Rehovot 7610001, Israel

Authors for correspondence:

Asaph Aharoni

Email: asaph.aharoni@weizmann.ac.il

Prashant Sonawane

Email: prashantsonawane@gmail.com

Received: 27 October 2021

Accepted: 7 February 2022

New Phytologist (2022) **234**: 1394–1410

doi: 10.1111/nph.18064

Key words: *Solanum*, specialized metabolism, steroidal glycoalkaloids (SGAs), structural diversity, tomato.

Summary

- *Solanum* steroidal glycoalkaloids (SGAs) are renowned defence metabolites exhibiting spectacular structural diversity. Genes and enzymes generating the SGA precursor pathway, SGA scaffold and glycosylated forms have been largely identified. Yet, the majority of downstream metabolic steps creating the vast repertoire of SGAs remain untapped.
- Here, we discovered that members of the 2-OXOGLUTARATE-DEPENDENT DIOXYGENASE (2-ODD) family play a prominent role in SGA metabolism, carrying out three distinct backbone-modifying oxidative steps in addition to the three formerly reported pathway reactions.
- The GLYCOALKALOID METABOLISM34 (GAME34) enzyme catalyses the conversion of core SGAs to habrochaitosides in wild tomato *S. habrochaites*. Cultivated tomato plants over-expressing GAME34 ectopically accumulate habrochaitosides. These habrochaitoside enriched plants extracts potently inhibit *Puccinia* spp. spore germination, a significant *Solanaceae* crops fungal pathogen. Another 2-ODD enzyme, GAME33, acts as a desaturase (via hydroxylation and E/F ring rearrangement) forming unique, yet unreported SGAs. Conversion of bitter α -tomatine to ripe fruit, nonbitter SGAs (e.g. esculeoside A) requires two hydroxylations; while the known GAME31 2-ODD enzyme catalyses hydroxytomatine formation, we find that GAME40 catalyses the penultimate step in the pathway and generates acetoxy-hydroxytomatine towards esculeosides accumulation.
- Our results highlight the significant contribution of 2-ODD enzymes to the remarkable structural diversity found in plant steroidal specialized metabolism.

Introduction

Plants produce a myriad of low molecular weight natural products with diverse functions in development, reproduction and defence. The remarkable structural diversity and associated biological activities of these metabolites result from extensive modifications of the core scaffold backbone, for example through oxidation, desaturation, hydroxylation, acylation, glycosylation, methylation and isomerization reactions. Among these modifications, oxygenation and hydroxylation reactions catalysed by cytochrome P450s (CYPs) and 2-oxoglutarate-dependent dioxygenases (2-ODDs) are widespread in both core and secondary

metabolisms (Farrow & Facchini, 2014; Kawai *et al.*, 2014; Islam *et al.*, 2018). Compared with CYPs, 2-ODDs have been studied to a lesser extent; however, members of this class catalyse a diverse array of oxidative reactions including demethylation, desaturation, halogenation, ring cleavage, ring rearrangement, ring closure and epimerizations (Farrow & Facchini, 2014; Hagel & Facchini, 2018). A typical plant genome contains >100 members of the 2-ODD family. These proteins are renowned for their activity in hormone biosynthetic and catabolic pathways (gibberellin and ethylene biosynthesis, auxin and salicylic acid catabolism) as well as in specialized metabolism *inter alia* flavonoid, glucosinolate, coumarin, benzoxazinoid and the

biosynthesis of various alkaloid classes (tropane, monoterpene indole, benzyloquinoline and steroidal alkaloids) (Farrow & Facchini, 2014; Kawai *et al.*, 2014).

Steroidal glycoalkaloids (SGAs) are defence specialized metabolites produced by hundreds of wild and cultivated *Solanum* species (Friedman, 2002, 2006; Cárdenas *et al.*, 2015; Sonawane *et al.*, 2020). The biosynthesis of SGAs precursor pathway (i.e. cholesterol), SGAs scaffold and glycosylated forms have been elucidated to a large extent (Itkin *et al.*, 2011, 2013; Cárdenas *et al.*, 2016, 2019; Sonawane *et al.*, 2016, 2018), yet the majority of downstream metabolic steps generating the immense structural diversity of this class remain untapped. To date, three distinct activities of 2-ODD enzymes have been associated with SGAs biosynthesis (Itkin *et al.*, 2013; Nakayasu *et al.*, 2017; Cárdenas *et al.*, 2019). In the core SGA biosynthetic pathway, GLYCOALKALOID METABOLISM11 (GAME11), a 2-ODD member catalyses the C-16 hydroxylation of 22,26-hydroxycholesterol to 16,22,26-hydroxycholesterol (Supporting Information Fig. S1). We recently reported on GAME31, a 2-ODD from tomato, that catalyses the C-23 hydroxylation of α -tomatine to hydroxytomatine (Cárdenas *et al.*, 2019); the first committed step towards the formation of the ripening-associated nonbitter SGAs (e.g. esculoside A) (Figs 1; S1). GAME32, a 2-ODD from wild potato species (*S. chacoense*), performs the C-23 hydroxylation of α -chaconine and α -solanine to form the Colorado potato beetle resistance-associated SGAs leptinine I and leptinine II, respectively (Cárdenas *et al.*, 2019) (Fig. S1). While enzymes of the CYPs family (i.e. GAME6, GAME8 and GAME4) catalyse hydroxylation/oxidation reactions in core SGAs biosynthesis (Itkin *et al.*, 2013) (Fig. 1, in blue), it is possible that downstream modifications in SGAs pathway require additional 2-ODD enzyme activities.

The occurrence and distribution of the various SGAs structures vary greatly between wild and cultivated species (Kozukue *et al.*, 2008; Iijima *et al.*, 2013; Schwahn *et al.*, 2014). Some SGAs are restricted to specific wild species and to cell or tissue types. For example, leptinines and leptines are foliar SGAs present only in the wild *Solanum chacoense* potato species (Mweetwa *et al.*, 2012). Similarly, torvoside A and torvoside H SGAs are unique to *Solanum torvum* (Eich, 2008). A different SGA, habrochaitoside A, is known to accumulate only in ripening fruit tissues of the wild tomato *Solanum habrochaites* (Iijima *et al.*, 2013; Schwahn *et al.*, 2014). While the steroidal A-D rings and sugar moieties of habrochaitoside A and α -tomatine are similar, the F ring of habrochaitoside A has a unique imine structure (C=N) (Fig. 1). For many years, habrochaitoside A formation in *S. habrochaites* was presumed to occur through oxidation of α -tomatine catalysed by cytochrome P450 enzymes (Iijima *et al.*, 2013; Schwahn *et al.*, 2014).

Here, we discovered that the involvement of the 2-ODD family in determining the structural variation of SGAs is even broader. We found that GAME34, a 2-ODD family enzyme, catalyses the conversion of α -tomatine to habrochaitoside A in *S. habrochaites*. Moreover, we identified another tomato 2-ODD family member (GAME33) that performs desaturation reaction on an array of SGA substrates forming unique SGAs not reported

so far. Additionally, in this study, we characterized a third 2-ODD enzyme, GAME40 that is involved in the biosynthetic pathway of nonbitter SGAs (e.g. esculoside A) downstream of α -tomatine in tomato. The prominent role of 2-ODD enzymes in SGAs modification highlights the key role of this enzyme class in generating the diversity and complexity of metabolites in plants, particularly in steroidal specialized metabolites.

Materials and Methods

Plant material

Twelve wild tomato accessions (*S. habrochaites* (LA1777 and LA0407), *S. chmielewskii* (LA1318, 732 and LA1028), *S. peruvianum* (PI126431 and PI126926), *S. pennellii* (LA0716), *S. pimpinellifolium* (LA1589 and LA1586) and *S. cheesmaniae* (LA1412 and LA1306)), selected introgression lines (ILs) (IL1-1, IL1-1-3 and IL2-1-1), backcross inbred lines (BILs) (#2033, #2357 and #2363), the two parental lines *S. lycopersicum* (cv M82) and *S. pennellii*, tomato varieties (*S. lycopersicum* cv Micro Tom and cv VF36), cultivated potato (*S. tuberosum* cv Desiree) and *S. chacoense* (accession no. 8380-1) plants were grown in a climate-controlled glasshouse at 24°C during the day and 18°C during night, with natural light. *Nicotiana benthamiana* plants were grown in a growth room maintained at 23 ± 2°C with 16-h : 8-h, day : night light regime.

LC-MS-based SGA analysis

Plant extracts preparations and targeted profiling of SGAs in various cultivated and wild tomato tissues (leaves, seeds at different developmental stages, flowers, roots, stems, green and red fruit) were performed as described previously (Itkin *et al.*, 2011; Cárdenas *et al.*, 2016, 2019; Sonawane *et al.*, 2018). Unless stated otherwise, at least three biological replicates from each genotype were used for metabolite analysis. Relative quantification of the SGA metabolites was carried out using the TargetLynx (Waters) program. The identification of habrochaitoside A SGA was confirmed by NMR studies. Detailed LC-MS methods and NMR spectroscopy are provided in Methods S1.

Transcriptome and quantitative real-time PCR analysis

RNA-seq libraries from four developmental stages of above-mentioned 12 wild tomato accessions were prepared and analysed as described previously (Jozwiak *et al.*, 2020). Targeted gene expression analysis was performed with three or more biological replicates ($n \geq 3$) for each genotype by qRT-PCR. Total RNA was isolated using the TRIzol method (Sigma-Aldrich). DNase I (Sigma-Aldrich)-treated RNA was reverse transcribed using a high-capacity cDNA reverse transcription kit (Applied Biosystems, Foster City, CA, USA). Gene-specific oligonucleotides were designed with PRIMER BLAST software (NCBI). The *TIP41* gene was used as an endogenous control in gene expression analysis.

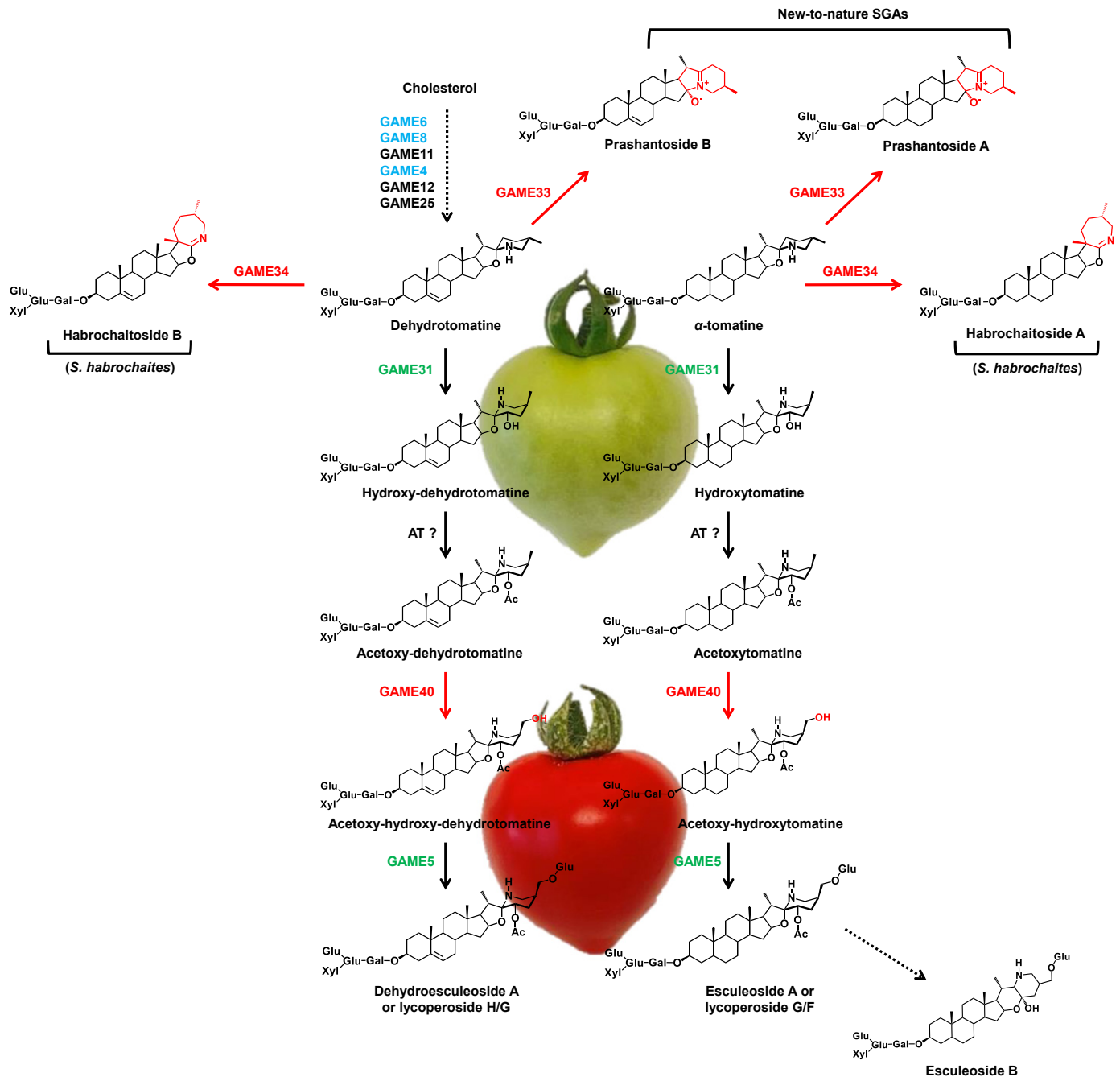


Fig. 1 Distinct 2-oxoglutarate-dependent dioxygenase (2-ODD) enzyme activities generate steroidal glycoalkaloids (SGAs) structural diversity in *Solanum* species. Steroidal glycoalkaloids pathway during tomato fruit development and ripening is presented here. The ripening-associated chemical shift in SGAs metabolism involves conversion of α -tomatine and dehydrotomatine (major SGAs in green fruit) to esculeoside A and dehydroesculeoside A, respectively. These represent major SGAs in red ripe fruit of cultivated tomato (e.g. *Solanum lycopersicum* cv M82 or Micro Tom) species. Conversely, habrochaitoside A and habrochaitoside B accumulate predominantly in the ripe fruit of *S. habrochaites*. The known SGA biosynthetic enzymes (i.e. GAME31 and GAME5) in the esculeoside A pathway are marked in green. Three known CYP enzymes involved in the core SGA pathway are presented in blue. GAME34, GAME33 and GAME40 enzymatic steps discovered in this study are shown in red. GAME34 from *S. habrochaites* catalyses the conversion of α -tomatine and dehydrotomatine to habrochaitoside A and habrochaitoside B, respectively, while GAME40 acts on acetoxytomatine to form acetoxy-hydroxytomatine in the esculeoside A biosynthetic pathway. GAME33 produces prashantose SGAs. Specific activity displayed by these GAME enzymes is shown in red on SGA structures. Dashed and solid arrows represent multiple and single biosynthetic reaction steps, respectively. GAME, GLYCOALKALOID METABOLISM; Glu, glucose; Gal, galactose; Xyl, xylose; Rha, rhamnose; Ac, acetoxy; AT, acyltransferase.

Escherichia coli expression and *in vitro* assays for GAME34, GAME33 and GAME40 enzymes

GAME34 genes from *S. habrochaites* (accession no. 1777; ShGAME34), *S. pennellii* (SpGAME34) and cultivated tomato (cv M82; SIGAME34) were cloned separately into the pET28b vector and expressed in *Escherichia coli* BL21 (DE3) cells. Soluble proteins were purified on Ni-NTA agarose beads (Adar Biotech, Rehovot, Israel) as described earlier (Cárdenas *et al.*, 2019). The recombinant GAME34 enzyme activity assay was performed according to Cárdenas *et al.* (2019) without any modifications. Enzyme assay products (habrochaitosides) were analysed by LC-MS. The detailed steps for GAME34, GAME33 and GAME40 proteins expression and their recombinant enzyme assays are provided in Methods S1.

GoldenBraid cloning and transient expression in *N. benthamiana* and tomato (cv VF36)

SbGAME34 and *SbGAME35* (from *S. habrochaites* accession no. 1777) overexpression constructs were generated using GoldenBraid cloning (Sarrion-Perdigones *et al.*, 2013). The *GAME34* and *GAME35* coding sequences were cloned separately into the pUPD1 vector and further moved into the respective 3 α 2 and finally to 3 Ω 1 vectors (pCAMBIA backbone-based). The respective 3 Ω 1 constructs harbouring either *SbGAME34* or *SbGAME35* were transiently expressed in *N. benthamiana* and tomato (cv VF36). Transient expression methods are described in Methods S1.

GAME34-VIGS in IL1-1 tomato plants

pTRV2 vector harbouring fragment of *GAME34* gene (cloned from IL1-1 line) was generated, and virus-induced gene silencing (VIGS) experiment was performed using selected IL1-1 tomato plants as described previously (Itkin *et al.*, 2009). VIGS experimental details are provided in Methods S1.

Generation of GAME33-Ox and GAME34-Ox transgenic tomato plants

StGAME33-Ox (cloned from cultivated potato), *ScGAME33-Ox* (cloned from *S. chacoense* accession no. 8380-1) and *SbGAME34-Ox* (from *S. habrochaites* accession no. 1777) constructs were prepared using GoldenBraid cloning as described above. 3 Ω 1:*SbGAME34*, 3 Ω 1:*StGAME33* and 3 Ω 1:*ScGAME33* constructs were transformed separately into tomato (cv Micro Tom) using *Agrobacterium tumefaciens* (strain GV3101)-mediated transformation (Cárdenas *et al.*, 2019). Positive transgenic lines were selected by qRT-PCR and further used for LC-MS-based prashantosides and other SGA analysis.

Phylogenetic analysis

GAME11, GAME31, GAME32, GAME33, GAME34, GAME35, GAME40 and their homologous sequences from

Solanum plants were retrieved using the BLASTP program (<https://blast.ncbi.nlm.nih.gov/Blast.cgi>). Sequence alignments were performed using CLUSTAL OMEGA (Sievers *et al.*, 2011). The maximum likelihood tree was inferred in MEGA6 using 1000 bootstrap replications (Tamura *et al.*, 2013). Amino acid sequences used in the phylogenetic analysis are provided in Dataset S1.

Fungal inhibition assay

Puccinia spp. fungal inhibition activity of *GAME34-Ox* and wild-type methanolic extracts was determined by a microplate-based method. The experiment was repeated at least three times. Details of fungal inhibition assay are described in Methods S1.

Results

Habrochaitoside A and B accumulate explicitly in ripening fruit of *S. habrochaites* among diverse wild tomato species

Iijima *et al.* (2013) isolated a novel SGA from ripe fruit of *S. habrochaites* (LA1777), which was termed habrochaitoside A and suggested its biosynthetic route to proceed through cytochrome P450-mediated hydroxylation of α -tomatine. We first employed liquid chromatography-mass spectrometry (LC-MS) and examined habrochaitoside A content in extracts of four fruit developmental stages (i.e. immature green, mature green, breaker and ripe) dissected from fruit of 12 wild tomato accessions. Habrochaitoside A (m/z 1032.55; C₅₀H₈₁NO₂₁) was detected merely in fruit of both *S. habrochaites* accessions (#1777 and #0407) (Fig. 2a) and not in any other wild species. Notably, gradual accumulation of habrochaitoside A was observed during the course of fruit ripening (Fig. 2a). In the same experiment, we detected the presence of a different, unreported SGA (m/z 1030.52, termed here habrochaitoside B; C₅₀H₇₉NO₂₁) that showed a similar accumulation pattern to the one of habrochaitoside A and appeared only in the two *S. habrochaites* accessions (Figs S2, S3). The level of habrochaitoside B was *c.* 6- to 10-fold lower than habrochaitoside A in the *S. habrochaites* accessions. We presumed that habrochaitoside B could likely be derived from dehydrotomatine. Apart from habrochaitoside A and B, we also detected a repertoire of other known SGAs associated with fruit ripening in both *S. habrochaites* accessions (e.g. α -tomatine, hydroxytomatine, acetoxytomatine and esculeoside A) (Fig. S4). To validate these observations, we further analysed ripening-associated SGAs in both *S. habrochaites* accessions in an independent experiment ($n=3$) (Fig. S5). Habrochaitoside A and B accumulation during the transition from green to ripe fruit was accompanied by a reduction in α -tomatine levels (Figs S4, S5). Furthermore, apart from fruit, we did not detect habrochaitosides (i.e. habrochaitoside A and B) in any other organ or tissue (e.g. leaves and flowers) of the *S. habrochaites* accessions. These results show that habrochaitoside A and B SGAs accumulate specifically in ripening fruit tissues of *S. habrochaites* accessions.

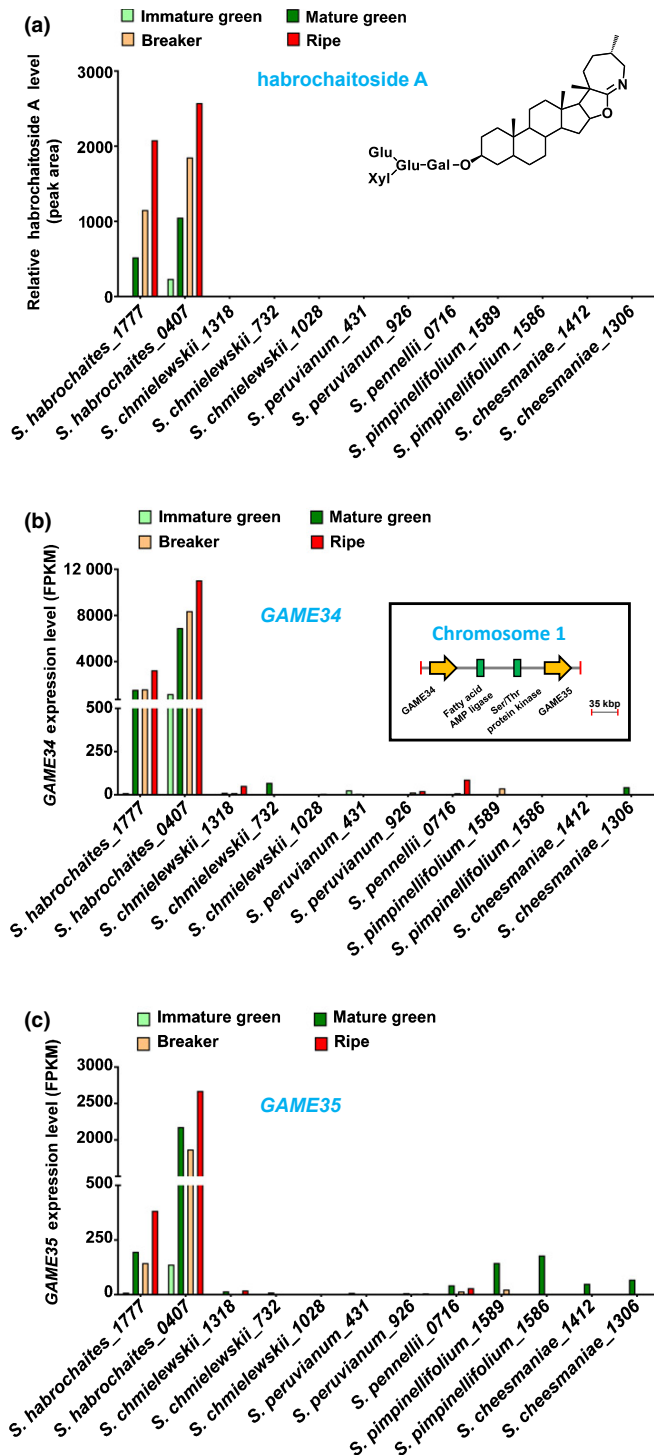


Fig. 2 Predominant accumulation of habrochaitoside A and expression of candidate *GAME34* and *GAME35* genes in ripe fruit of the wild tomato species *Solanum habrochaites*. (a) Liquid chromatography-mass spectrometry (LC-MS)-based profiling of habrochaitoside A in different wild tomato species during four stages of fruit development ($n = 1$, single replicate for each fruit developmental stage was prepared by grinding several fruits from individual wild tomato species). (b, c) *GAME34* (b) and *GAME35* (c) expression levels in four fruit developmental stages of wild tomato accessions (normalized RNA-seq data). Inset in (b) displays the genomic organization of *GAME34* and *GAME35* on chromosome 1. FPKM, fragments per kilobase of transcript per million mapped reads.

Identification of candidate genes involved in habrochaitoside A biosynthesis

For many years, the biosynthesis of habrochaitoside A from α -tomatine was anticipated to occur via an oxidation step catalysed by a cytochrome P450 enzyme. We envisaged that as for habrochaitoside A, a similar oxidation step and corresponding enzyme might be required to form habrochaitoside B from dehydrotomatine. To discover gene(s) associated with habrochaitosides biosynthesis, we generated transcriptomic data from four fruit developmental stages of the above-mentioned 12 wild tomato accessions. Next, we searched for candidate genes based on their predominant and elevated expression in the breaker and ripe stages of *S. habrochaites* accessions (i.e. #1777 and #0407) as compared to fruit of other wild accessions. While no CYPs genes matched our selection criteria, two putative 2-ODD genes displayed a pertinent expression profile. Both genes termed here *GLYCOALKALOID METABOLISM34* (*GAME34*, Solyc01g006580) and *GLYCOALKALOID METABOLISM35* (*GAME35*, Solyc01g006610) were found to be located in close proximity (in a *c.* 35 kbp region on chromosome 1) flanking two other genes (see inset in Fig. 2b) and shared 90% homology at amino acid level. *GAME34* and *GAME35* genes were predominantly expressed in ripening fruit tissues of *S. habrochaites* accessions (Fig. 2b,c) resembling the profile of habrochaitoside A and B (Figs 2a, S2). The results suggested that *GAME34* and *GAME35* genes could take part in habrochaitosides biosynthesis in *S. habrochaites* fruit.

Habrochaitosides accumulate in young seedlings of cultivated tomato and leaves of the wild species *Solanum pennellii*

It has been suggested that habrochaitosides SGAs are produced only in fruit of *S. habrochaites* and not in any tissues of wild and cultivated tomato varieties (Iijima *et al.*, 2013). Here, we surveyed habrochaitoside A content in different tissues of cultivated tomato (*S. lycopersicum* cv Micro Tom) at three developmental time points: seedling (7 and 15 d old), young (4–6 wk old) and old (8–10 wk old) plants. We could not detect habrochaitosides in any of the analysed tissues (leaves, stem, green fruits and red fruit) from 8- to 10-wk-old tomato plants (Fig. S6a). Yet, we discovered high accumulation of habrochaitoside A in roots, hypocotyl and cotyledons of 7-d-old and 15-d-old tomato seedlings (Fig. S6a). We also detected habrochaitoside A in stem and roots, but not in leaves of young (4- to 6-wk-old) tomato plants. Thus, habrochaitoside A is indeed produced by cultivated tomato species at early stages of plant development.

While searching an in-house transcriptomics data of cv Micro Tom (Cárdenas *et al.*, 2016), we found that both *GAME34* and *GAME35* candidate genes were expressed in seeds of different fruit developmental stages. Apart from this, no other tissue examined (i.e. leaves (4-wk-old), petals, buds, as well as skin and flesh tissues derived from fruit at various developmental stages) showed detectable *GAME34* or *GAME35* expression (Fig. S6b,c). Despite *GAME34* and *GAME35* expression in seeds, we could not detect habrochaitosides in mature and ripe fruit seeds of cultivated tomato (cv Micro Tom).

Interestingly, unlike *S. habrochaites* and cultivated tomato varieties (cv M82 and cv Micro Tom), we found that leaves (4- to 6-wk-old) of the wild species *S. pennellii* do accumulate habrochaitoside A and B (Fig. 3a). The results provided here clearly show that habrochaitosides accumulation is not exclusive to ripening fruit tissues of *S. habrochaites*.

Analysis of introgression lines indicates that *GAME34* and not *GAME35* is associated with habrochaitosides biosynthesis

The presence of habrochaitosides in *S. pennellii* leaves prompted us to correlate genotype to chemotype in tomato-

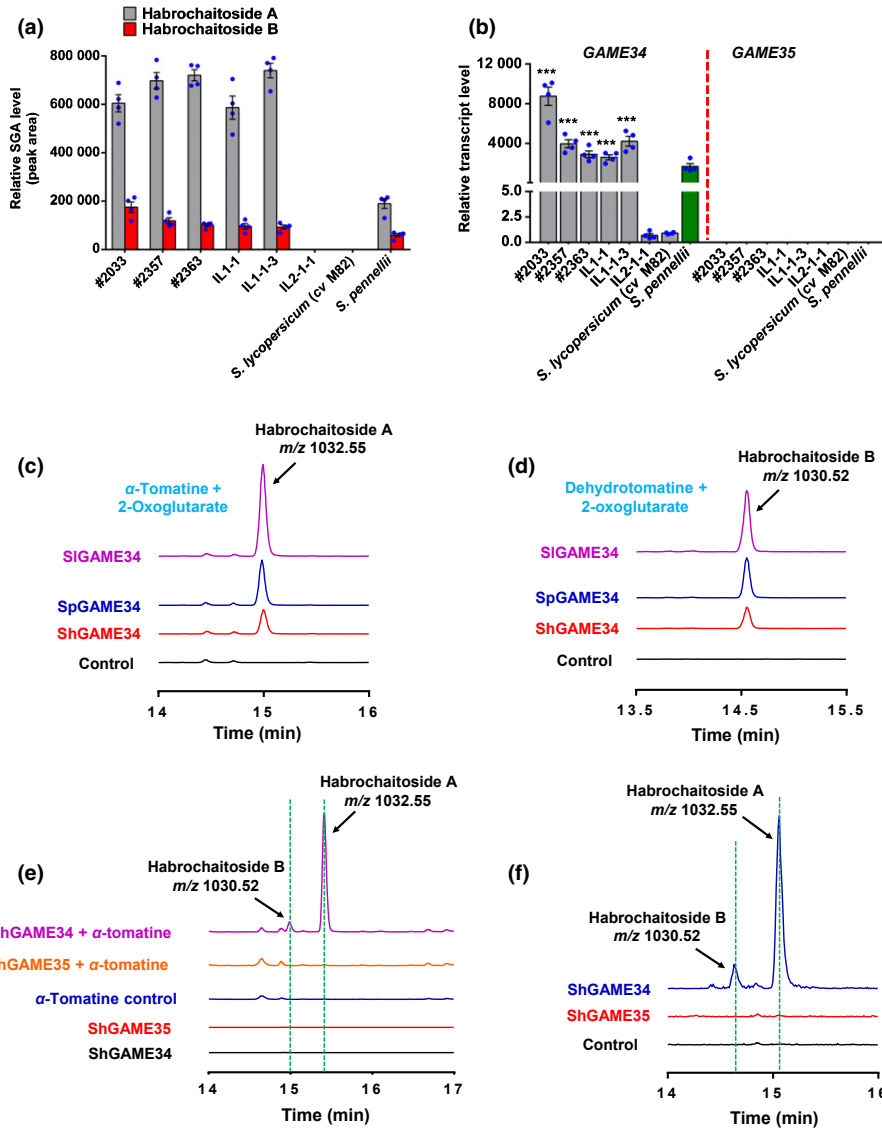


Fig. 3 *In vitro* and *in planta* assays confirm the role of *GAME34* and not *GAME35* in habrochaitosides biosynthesis. (a) Habrochaitoside A and habrochaitoside B content in leaf tissue extracts of selected backcross inbred lines (BILs), introgression lines (ILs) along with *Solanum lycopersicum* (cv M82) and wild species (*S. pennellii*) parents. (b) *GAME34* and *GAME35* expression levels in leaves of selected BILs, ILs and the parents (*S. lycopersicum* (cv M82) and *S. pennellii*) as determined by quantitative real-time PCR (qRT-PCR). The values in (a, b) indicate means of four biological replicates \pm SE mean ($n = 4$). Asterisks in (b) indicate a significant difference from *S. lycopersicum* samples calculated by a Student's *t*-test (***, $P < 0.001$). IL2-1-1 line was used as negative control. LC-MS was used for targeted steroidal glycoalkaloids (SGAs) analysis. (c, d) Recombinant ShGAME34 (*S. habrochaites* (accession no. 1777); shown in red), SpGAME34 (*S. pennellii*, in blue) and SIGAME34 (*S. lycopersicum* (cv M82); in pink) enzymes (produced separately in *Escherichia coli* cells) convert α -tomatine (c) and dehydrotomatine (d) to habrochaitoside A and habrochaitoside B, respectively. The control reaction (in black) contained the respective substrate and the protein extracts of empty vector-transformed *E. coli* cells. Mass to charge (m/z) is shown for assay products (i.e. habrochaitosides). Enzyme assays analysis was carried out by LC-MS. (e) Extracted ion chromatograms (EICs) of habrochaitoside A (m/z 1032.55) and habrochaitoside B (m/z 1030.52) from *Nicotiana benthamiana* leaf extracts expressing ShGAME34 or ShGAME35, with and without infiltration of α -tomatine (the commercial standard contains dehydrotomatine as an impurity). Transient expression of ShGAME34 in *N. benthamiana* leaves produces habrochaitoside A and habrochaitoside B, typically not generated in *N. benthamiana* leaves. (f) Transient expression of ShGAME34 in tomato (cv VF36) resulted in habrochaitoside A and habrochaitoside B production. For (e, f), EIC results from LC-MS analysis are shown.

inbred populations (ILs and BILs). Both ILs and BILs are derived from crosses between the cultivated *S. lycopersicum* cv M82, and the wild species *S. pennellii* LA0716. Each line possesses either a single (in the case of the ILs) or multiple (in BILs) chromosomal regions introgressed from *S. pennellii* into the M82 background (Eshed & Zamir, 1995; Ofner *et al.*, 2016). In recent years, screening of these populations to map quantitative trait loci (QTLs) appeared as a powerful approach (Alseikh *et al.*, 2015; Ofner *et al.*, 2016; Szymanski *et al.*, 2020). Here, we employed a reverse approach to the one typically employed and focused our investigation on particular BILs and ILs covering the introgression region that includes our gene(s) of interest (i.e. *GAME34* and *GAME35*). Thus, we selected three BILs (#2033, #2357 and #2363) and two ILs (IL1-1 and IL1-1-3) that might display altered habrochaitosides content due to introgression in chromosome 1 spanning the *GAME34* and *GAME35* gene loci. To test this, we measured habrochaitosides content in leaves of the selected ILs, BILs and the parental lines. Habrochaitoside A and habrochaitoside B were not detected in leaves of *S. lycopersicum* (cv M82) and IL2-1-1 (serving as a negative control), while those of the *S. pennellii* parent accumulated these SGAs (Fig. 3a). Leaves of selected ILs (IL1-1 and IL1-1-3) and BILs (#2357, #2363 and #2033) displayed notable accumulation of habrochaitoside A and habrochaitoside B, even higher than in the *S. pennellii* parent (Figs 3a, S7a). These results suggested that *GAME34* and/or *GAME35* are linked to the increase in habrochaitoside content.

Next, we compared *GAME34* and *GAME35* expression levels in leaves of the investigated genotypes and could not detect *GAME35* expression in any of the samples (Fig. 3b). *GAME34* showed negligible expression in leaf tissue of the cultivated tomato (cv M82) and IL2-1-1 correlating with the lack of habrochaitosides in the leaves of these genotypes (Fig. 3a,b). With similarity to *S. pennellii*, the selected BILs (#2033, #2357 and #2363), IL1-1 and IL1-1-3 lines displayed high *GAME34* expression (Fig. 3b), correlating with the presence of high habrochaitoside levels in these lines (Figs 3a, S7a). We also examined the expression of *GAME34* and *GAME35* genes across the core IL population (obtained from a previously reported leaf transcriptome data of the ILs population, Chitwood *et al.*, 2013). It appeared that only *GAME34* was expressed in the IL population and showed differential expression in leaves of IL1-1 and IL1-1-3 across the entire ILs set (Fig. S7b). Furthermore, we also measured *GAME34* expression in different tissues of cultivated tomato (cv Micro Tom) at 7-d seedling, 4- to 6-wk-old and 8- to 10-wk-old stages. *GAME34* displayed predominant expression in roots and hypocotyls of 7-d-old seedlings as well as in stem and roots of 4- to 6-wk-old tomato plants (Fig. S8). The *GAME34* expression pattern strongly resembled the profile of habrochaitoside A, which accumulated mainly in the same tissues (Fig. S6a). Hence, these results indicated that *GAME34* and most likely not *GAME35* are associated with habrochaitoside accumulation in cultivated and wild tomato (*S. pennellii*) varieties.

Recombinant GAME34 enzymes produce habrochaitoside A from α -tomatine *in vitro*

To establish the role of *GAME34* enzyme in habrochaitoside biosynthesis, we expressed the *GAME34* genes from *S. habrochaites* (accession no. 1777; Sh*GAME34*), *S. pennellii* (Sp*GAME34*) and cultivated tomato (cv M82; Si*GAME34*) in *E. coli* cells. We performed enzyme activity assays with different steroidal alkaloid (SA) and steroidal glycoalkaloid (SGA) substrates that are typically found in tomato (e.g. tomatidine, α -tomatine and dehydrotomatine) and potato (e.g. solanidine, α -solanine and α -chaconine). Incubation of each of the three *GAME34* recombinant enzymes with α -tomatine (m/z 1034.55) as a substrate in the presence of α -ketoglutarate, ascorbate and Fe^{2+} yielded habrochaitoside A (m/z 1032.55) (Fig. 3c). Moreover, the recombinant *GAME34* enzymes also produced habrochaitoside B (m/z 1030.52) when assayed using dehydrotomatine (m/z 1032.55) as a substrate (Fig. 3d). The habrochaitoside A and habrochaitoside B LC-MS mass spectra observed in these experiments were identical to the ones detected in the leaves of *S. pennellii*, IL1-1 and ripe fruit extracts of *S. habrochaites* (accession no. 1777) (Fig. S9a). The Si*GAME34* and Sh*GAME34* recombinant enzymes also acted on tomatidine (m/z 416.3), aglycone of α -tomatine to form a compound (termed here habrochaitoside C) with mass m/z 414.3 (Fig. S9b). Interestingly, none of the *GAME34* enzymes (Si*GAME34* or Sh*GAME34* or Sp*GAME34*) was active with the tested potato alkaloids, that is the solanidane type, α -solanine, α -chaconine and solanidine. We also examined the activity of recombinant *GAME35* (*S. habrochaites* accession no. 1777; Sh*GAME35*) using a similar set of SAs and SGAs substrates. The recombinant Sh*GAME35* enzyme was not active with any of the tomato and potato SAs and SGAs substrates. Taken together, the results confirm the role of *GAME34* enzyme in habrochaitoside biosynthesis. The structure of habrochaitoside A observed in the selected ILs/BILs, recombinant enzyme assays and ripe fruit extracts of *S. habrochaites* plants was unambiguously determined using nuclear magnetic resonance (NMR) analysis (Table S1; Notes S1–S7).

GAME34 catalyses formation of habrochaitosides *in planta*

To test the *in vivo* activity of Sh*GAME34*, we used *Agrobacterium*-mediated transient expression in *Nicotiana benthamiana* (*N. benthamiana*) leaves. We infiltrated *N. benthamiana* leaves with either Sh*GAME34* or Sh*GAME35* and, 3 d later, infiltrated the same leaves with α -tomatine substrate. Leaves collected 2 d following substrate feeding were analysed by LC-MS. We detected habrochaitoside A and habrochaitoside B in leaves infiltrated with Sh*GAME34* (Fig. 3e) but not in Sh*GAME35* (from *S. habrochaites* accession no. 1777) and agroinfiltrated leaves (either with *GAME34* or *GAME35*) but without α -tomatine supplementation. We also infiltrated and transiently expressed Sh*GAME34* and Sh*GAME35* in leaves of 4- to 5-wk-old tomato plants. The VF36 cultivar was used as it lacks habrochaitosides, produces the required substrates (i.e. α -tomatine and dehydrotomatine) and is amenable to

agroinfiltration experiments in contrast to other cultivars used in this study. The expression of *SbGAME34* in VF36 leaves resulted in the formation of habrochaitoside A and B (Fig. 3f). However, these SGAs were not detected in the case of *ShGAME35* infiltrated leaves. Altogether, the results show that the *GAME34* enzyme is capable of catalysing habrochaitosides biosynthesis in plants.

As shown above, leaves of selected IL express *GAME34* and produce habrochaitosides (Fig. 3a,b). We employed virus-induced gene silencing (VIGS) to examine the consequence of reduced *GAME34* expression on SGAs levels in a representative IL (i.e. IL1-1) (Fig. S10a). *GAME34*-VIGS-silenced IL1-1 leaves showed a significant reduction in habrochaitoside A and B levels (Fig. S10b). While levels of the α -tomatine (the habrochaitoside A precursor) increased mildly, we observed a significant increase in hydroxytomatine, an SGA downstream of α -tomatine in the *GAME34*-silenced IL1-1 leaves (Fig. S10c).

Overexpression of *GAME34* in cultivated tomato resulted in accumulation of habrochaitoside A

Many tissues of cultivated tomato (e.g. leaves and fruits) do not produce habrochaitosides. To examine the impact of *GAME34* activity in cultivated tomato, we generated transgenic tomato lines (cv Micro Tom) overexpressing the *SbGAME34* gene (from *S. habrochaites*) (Fig. S11a). Leaves and green fruits of *GAME34*-overexpressing (*GAME34*-Ox) tomato plants showed *de novo* accumulation of habrochaitoside A (Fig. S11b). Moreover, *GAME34*-Ox did not affect normal growth and development of transgenic tomato lines compared to wild-type tomato plants.

Habrochaitosides enriched leaf extracts inhibit tomato fungal pathogen spore germination

SGAs are known to function in the plant defence against a wide range of pathogens and predators, including bacteria, fungi, viruses, insects and animals (Friedman, 2002; Sonawane *et al.*, 2018). Although α -tomatine, a major SGA in cultivated tomato, plays a protective role against various pathogenic fungi, the role of habrochaitoside A in phytopathogenicity remains unclear. As overexpression of *GAME34* in cultivated tomato resulted in *de novo* accumulation of habrochaitoside A in leaves, we tested the effects of habrochaitoside A enriched *GAME34*-Ox leaf extracts against various bacterial (*Pectobacterium* spp., *Pseudomonas* spp. and *Xanthomonas* spp.) and fungal (*Alternaria* spp., *Botrytis* spp., *Fusarium* spp., *Phytophthora* spp., *Puccinia* spp., *Pythium* spp. and *Rhizoctonia* spp.) pathogens. Among several pathogens tested, *GAME34*-Ox extracts showed notable 'antifungal' activity against spore germination of *Puccinia* spp., an important fungal pest of *Solanaceae* crops. While *GAME34*-Ox leaf extracts showed complete inhibition of *Puccinia* spore germination as comparable to the ones observed when treated with commercial fungicides, no germination inhibition was observed for wild-type extracts typically enriched with α -tomatine (Fig. S12).

Phylogenetic analysis reveals *GAME33* as a different 2-ODD-type enzyme associated with steroidal glycoalkaloids metabolism

Phylogenetic analysis of the various 2-ODD *GAME* proteins involved in SGA metabolism revealed that members of the same subclade catalyse similar reactions (Fig. 4). *GAME31* proteins performing C-23 hydroxylation of spirosolane type SGAs (from tomato and eggplant) form a separate clade (Clade I, red in Fig. 4), while *GAME34* proteins involved in habrochaitosides (habrochaitoside A and B) biosynthesis form a distinct subclade related to the *GAME31* clade (Clade II, light blue in Fig. 4). The *GAME11* proteins participating in core SGA pathway and catalysing C-16 hydroxylation of the cholesterol backbone (i.e. 22,26-hydroxycholesterol) are clearly separated from the rest of the 2-ODD *GAME* proteins further modifying core SGAs, suggesting early evolution of their unique catalytic activity in SGAs biosynthesis (clade III, purple in Fig. 4). *GAME32* proteins from *S. chacoense* (wild potato) possessing C-23 hydroxylation activity that is specific to solanidane type SAs and SGAs (from potato) form a distinct clade in the phylogeny (clade IV, blue in Fig. 4). Interestingly, another clade of 2-ODD family members from various *Solanum* species (termed here *GAME33*) forms a large separated clade that likely shares a common ancestor with the *GAME32* proteins (Clade V, orange in Fig. 4). Despite 70% to 85% homology (at the amino acid level) with *GAME32* proteins, individual recombinant assay of *GAME33* enzymes from tomato (*SIGAME33*; Solyc00g138060), potato (*StGAME33*), *S. chacoense* (*ScGAME33*; cloned from accession no. 8380-1) and *S. pennellii* (*SpGAME33*) failed to show any hydroxylase activity with either potato (solanidine type), or with tomato (spirosolane type) SAs and SGAs substrates. Clear separation of the *GAME33* clade from the *GAME11*, *GAME31*, *GAME32* and *GAME34* clades and lack of hydroxylation activity of its members suggested a unique function for *GAME33* enzymes likely in SGAs metabolism. Two other 2-ODD members, *StGAME32*-like (from cultivated potato) and *ScGAME32*-like (from wild potato) that are homologs of *ScGAME32*, did not show hydroxylase activity with any tested tomato or potato SAs or SGAs substrates. These two proteins appeared between the *GAME33* and *GAME32* subclades in the phylogenetic analysis.

Recombinant *GAME33* enzymes produce yet unknown desaturated steroidal glycoalkaloids

We next examined the expression of *GAME33* in four fruit developmental stages of 12 wild tomato accessions and different tissues of the cultivated tomato. *GAME33* expression was at trace levels in all wild species (FPKM < 10) (Fig. S13a). In cultivated tomato (cv Micro Tom), *GAME33* displayed weak expression in seeds of mature green and red, ripe fruit (FPKM < 15; RNA-seq expression data, Cárdenas *et al.*, 2016) (Fig. S13b).

To determine the possible role of *GAME33* in SGA metabolism, we expressed *SIGAME33* (from the cultivated tomato (cv Micro Tom)) and *SpGAME33* (from *S. pennellii*) separately in *E. coli* cells and performed enzyme assays with different

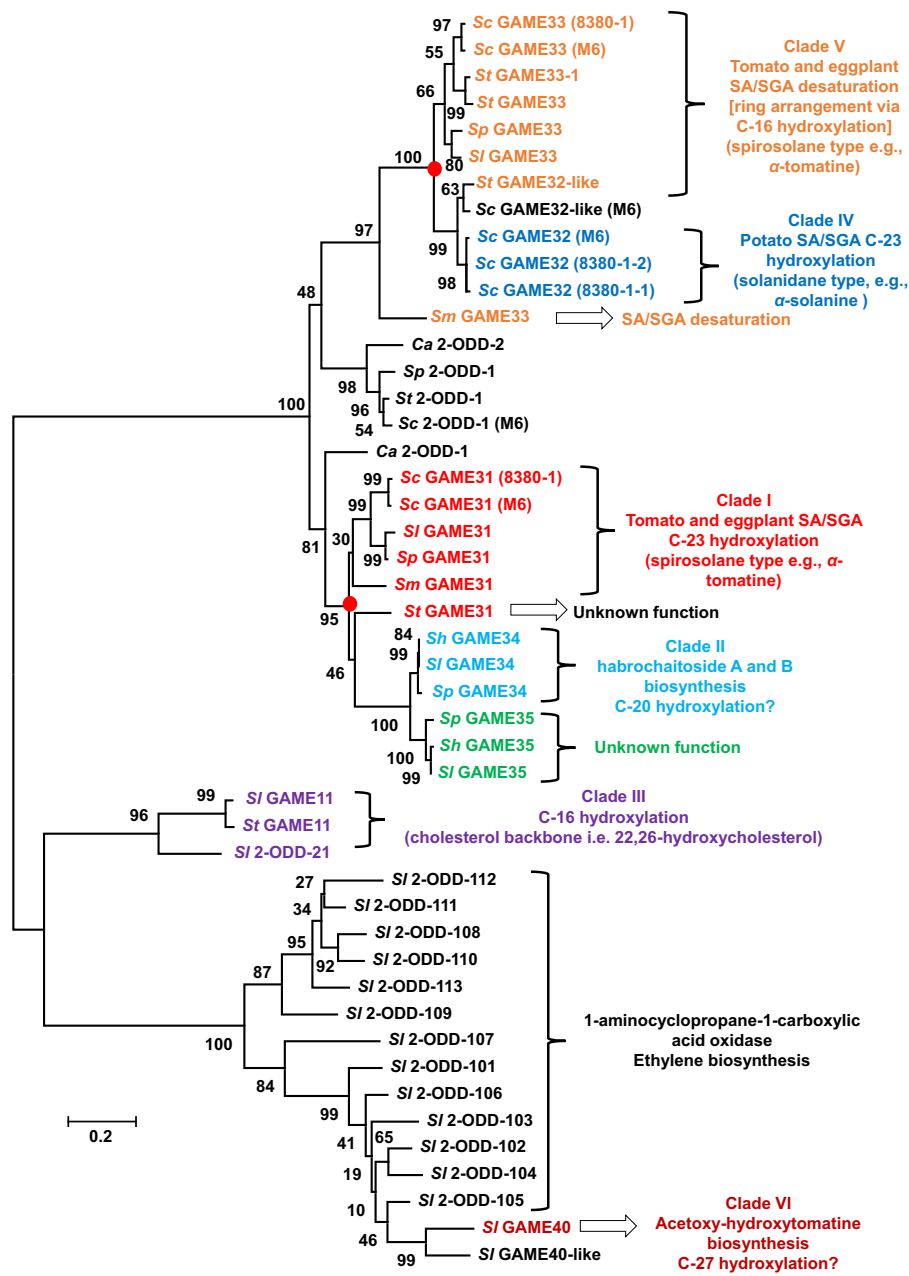


Fig. 4 Phylogenetic analysis clusters 2-ODD GAME proteins according to their activity in steroidal glycoalkaloid (SGA) metabolism. The protein sequences used in the phylogeny are from the following *Solanum* species: cultivated tomato (*S. lycopersicum* (*Sl*)), cultivated potato (*S. tuberosum* (*St*)), wild tomato (*S. pennellii* (*Sp*)), *Capsicum annuum* (*Ca*), cultivated eggplant (*S. melongena* (*Sm*)), wild potato (*S. chacoense* (*Sc*), accession no. M6 and #8380-1). GAME11, GAME31, GAME32, GAME33, GAME34, GAME35 and GAME40 proteins forming separate clades are depicted in purple, red, blue, orange, light blue, green and dark red colours, respectively. Numbers are bootstrap values in percentage of 1000 replicates. Amino acid sequences used in the phylogenetic analysis are provided in Supporting Information Dataset S1. Red dot denotes a common ancestor shared between respective GAME proteins in the clade. Evolutionary history was inferred using the maximum-likelihood method in MEGA6.0 using 1000 bootstrap replications.

sets of SAs and SGAs substrates. Both SlGAME33 and SpGAME33 recombinant enzymes generated a new product, that we termed prashantoside A (m/z 1032.55; $C_{50}H_{81}NO_{21}$) when incubated with α -tomatine (m/z 1034.55; $C_{50}H_{83}NO_{21}$) as a substrate (Fig. 5a). The m/z shift between prashantoside A and the substrate fragment ions was 2 Da, suggesting direct desaturation reaction (addition of a double bond) rather than the expected 16 Da representing hydroxylation. Alternatively, we also hypothesized that initial hydroxylation (16 Da) followed by ring rearrangement (through loss of H_2O , -18 Da) could also result in desaturation mechanism and generate a corresponding desaturated compound, for example prashantoside A from α -tomatine. Although prashantoside A has the same molecular formula as habrochaitoside A and dehydrotomatine, the

retention time and mass spectra (Fig. S14) of these compounds are different. The SlGAME33 recombinant enzyme could also catalyse the reactions forming prashantoside B (m/z 1030.54; $C_{50}H_{79}NO_{21}$), prashantoside C (m/z 414.33; $C_{27}H_{43}NO_2$), prashantoside D (m/z 412.33; $C_{27}H_{41}NO_2$) and prashantoside E (m/z 866.5; $C_{45}H_{71}NO_{15}$) from dehydrotomatine (m/z 1032.54; $C_{50}H_{81}NO_{21}$), tomatidine (m/z 416.33; $C_{27}H_{45}NO_2$), solasodine (eggplant alkaloid aglycone; m/z 414.33; $C_{27}H_{43}NO_2$) and α -solamargine (eggplant SGA; m/z 868.5; $C_{45}H_{73}NO_{15}$), respectively (Fig. 5b–e). The enzyme from *S. pennellii* (SpGAME33) was also able to produce prashantoside B (Fig. 5b) and prashantoside E (Fig. 5e) *in vitro* when incubated with dehydrotomatine and α -solamargine, respectively. The chemical structures of prashantoside SGAs identified here are shown in Fig. S15.

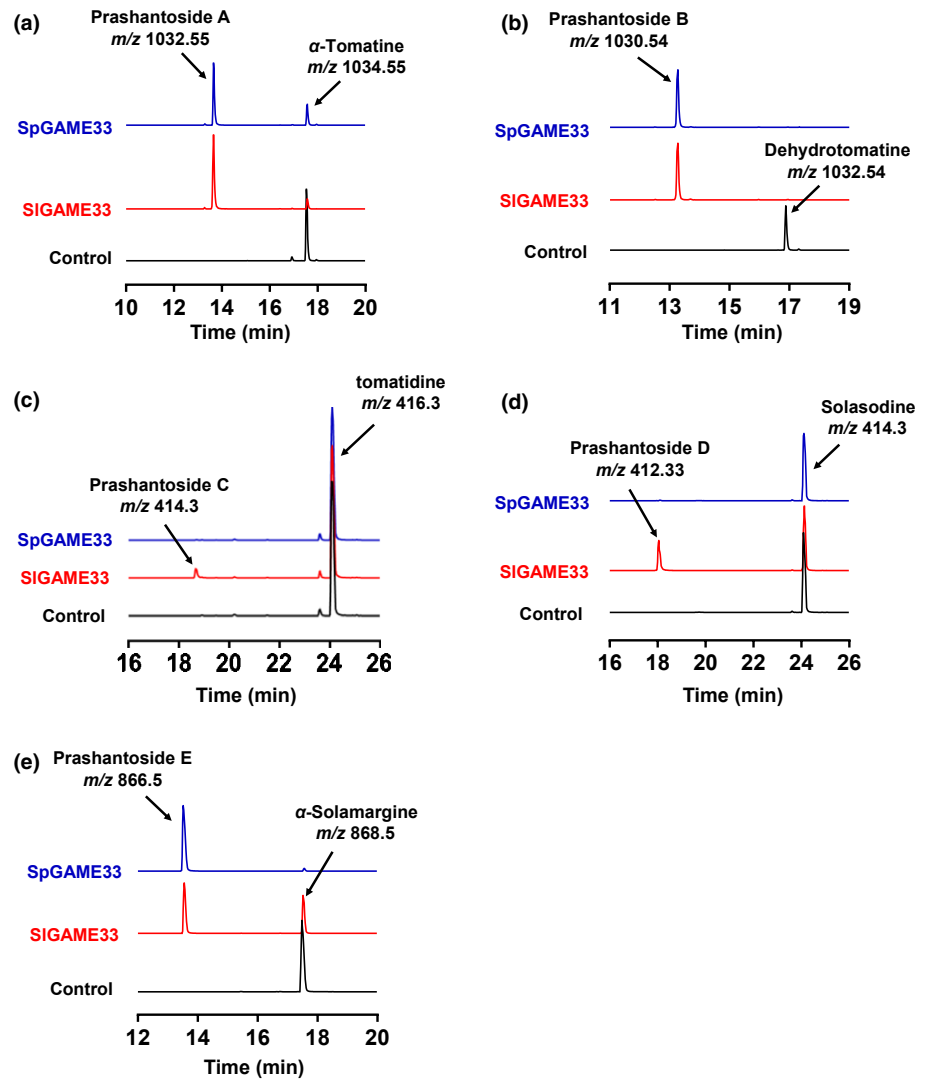


Fig. 5 Recombinant GAME33 enzyme(s) produce desaturated prashantosiol glycoalkaloids (SGAs). The cultivated tomato GAME33 (SIGAME33) and wild tomato species *Solanum pennellii* GAME33 (SpGAME33) proteins were expressed separately in *Escherichia coli* cells. (a–e) Aligned extracted ion chromatograms (EICs) of desaturated products (i.e. prashantosiol SGAs) in SIGAME33 (red), SpGAME33 (dark blue) assays and a control reaction (in black; protein extracts from *E. coli* cells harbouring empty vector). Enzyme assays performed with the following substrates: α -tomatine (a), dehydrotomatine (b), tomatidine (c), solasodine (d) and α -solamargine (e). *m/z*, mass to charge. Putative identification of desaturated compounds (GAME33 assay products) by MS-MS analysis is provided in Supporting Information Fig. S15.

We next identified the putative homologs of tomato GAME33 in eggplant (SmGAME33), cultivated potato (StGAME33) and wild potato *S. chacoense* accession no. 8380-1 (ScGAME33 (8380-1)). It appeared that all these recombinant GAME33 enzymes possess desaturation activity when incubated with the set of SAs and SGAs substrates, forming prashantosiol SGAs (Figs S16–S18). However, none of the recombinant GAME33 enzymes showed desaturation activity with the typical potato solanidine type SA and SGA substrates. Moreover, the StGAME32-like enzyme from cultivated potato (refer to the phylogeny in Fig. 4) was also able to produce prashantosiol SGAs *in vitro* when assayed with tomato and eggplant SAs and SGAs (spirosolane type) substrates (Fig. S19). As observed for GAME33 enzymes, StGAME32-like enzyme was also not active with any potato SA and SGA substrates. During the course of this study, a different group reported DPS (dioxygenase for potato solanidine synthesis; the StGAME32-like enzyme reported here) characterization from potato. Akiyama *et al.* (2021) showed that DPS catalyses the

C-16 hydroxylation of spirosolane type SGAs (e.g. α -solamargine) that results in desaturation via E/F ring arrangement to form the potato-specific solanidine type backbones. MS-MS analysis of prashantosiols A–E shown here (formed by action of GAME33 and StGAME32-like recombinant enzymes) suggests desaturation via hydroxylation and rearrangement of E/F ring, resulting in the same major fragment *m/z* 162.31 (Fig. S15) in all prashantosiol metabolites discovered here (i.e. prashantosiols A–E).

We searched for prashantosiol SGAs in different wild and cultivated *Solanum* species including tomato, potato and eggplant, and could not find these SGAs natively in any of the *Solanum* species investigated. Moreover, seeds of different fruit developmental stages of cultivated tomato (cv Micro Tom) do not accumulate prashantosiol SGAs albeit showing very weak GAME33 expression levels in seeds (Fig. S13b). Thus, our results indicate that GAME33 clade proteins from *Solanum* species generate a range of yet unreported, possibly ‘new to nature’, desaturated SAs and SGAs.

De novo production of prashantosi- de SGAs by overexpression of *GAME33* in tomato

Following our finding that *GAME33*, a 2-ODD enzyme produces prashantosi-*de* SGAs *in vitro* through desaturation reaction, we assessed whether this enzyme will generate such SGAs in tomato plants. We generated stable transgenic tomato lines (cv Micro Tom) overexpressing either *StGAME33* (termed *StGAME33-Ox*; cloned from cultivated potato) or *ScGAME33* (termed *ScGAME33-Ox*; cloned from *S. chacoense* accession no. 8380-1) genes. Overexpression of *StGAME33* and *ScGAME33* genes in different tissues (i.e. leaves, green fruit and red fruit) was confirmed by analysing transgene expression (Fig. S20). We observed *de novo* production of prashantosi-*de* A, prashantosi-*de* B and their isomers in leaves of *StGAME33-Ox* plants (Figs S21a, S22). *StGAME33-Ox* leaves did not show significant change in α -tomatine levels; however, we observed reduction in dehydrotomatine, hydroxytomatine, acetoxytomatine and α -tomatine isomer levels in the same tissue (Fig. S21b). Consistent with *StGAME33-Ox* results, we also detected the accumulation of prashantosi-*de* SGAs in *ScGAME33-Ox* leaves (Figs S21c, S22). No effect on α -tomatine levels albeit concomitant reduction in other downstream SGAs was also noted in *ScGAME33-Ox* leaves (Fig. S21d).

During the transition from green to red fruit, α -tomatine and dehydrotomatine are typically converted to esculeosides (e.g.

esculeoside A) and dehydroesculeosides (e.g. dehydroesculeoside A), respectively (Fig. 1 for tomato SGA pathway). Green fruit of both *StGAME33-Ox* and *ScGAME33-Ox* lines displayed reduction in α -tomatine-, α -tomatine isomer-, dehydrotomatine- and α -tomatine-derived downstream SGAs (i.e. acetoxytomatine and acetoxy-hydroxytomatine) as compared to wild-type green fruit (Figs S23a,c, S24a). By contrast, we detected high levels of prashantosi-*de* A, prashantosi-*de* B and their isomers in *StGAME33-Ox* and *ScGAME33-Ox* green fruit (Figs S23b,d, S24a). Thus, overexpression of *GAME33* in tomato green fruit resulted in a metabolic shift from production of α -tomatine- and dehydrotomatine-derived SGAs to prashantosi-*de* SGAs biosynthesis.

Compared to wild-type fruit, *StGAME33-Ox* or *ScGAME33-Ox* red, ripe fruit displayed substantial reduction in esculeoside A (c. 9- to c. 25-fold), the major SGA in red fruit of cultivated tomato (Fig. 6a,c). Furthermore, we found that several other SGAs produced downstream of α -tomatine towards esculeoside A were substantially reduced as compared to wild-type red fruit (Fig. 6a,c, S25 and refer to Fig. 1 for SGA pathway). Prashantosi-*de* A, prashantosi-*de* B and their isomers were the predominant SGAs in red fruit of *StGAME33-Ox* or *ScGAME33-Ox* tomato plants (Figs 6b,d, S24b). Notably, we did not detect further modification of prashantosi-*de* SGAs in any of the tissues (leaves, green fruit and red ripe fruit) examined from *StGAME33-Ox* or *ScGAME33-Ox* tomato plants. It is likely that

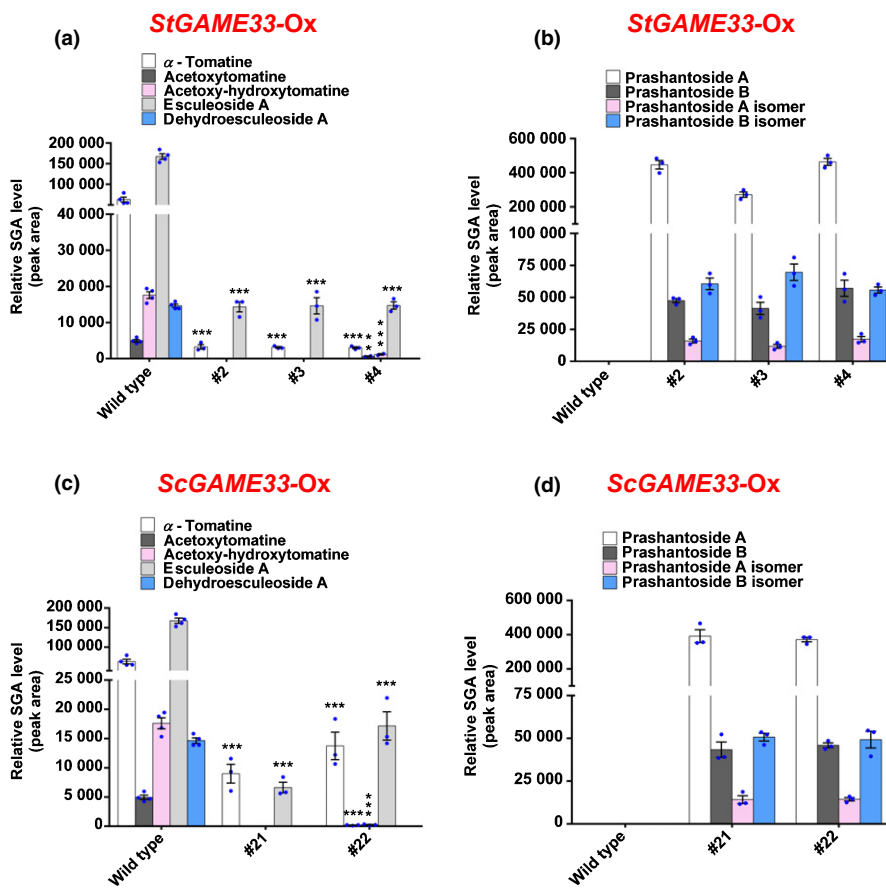


Fig. 6 Prashantosi-*de* steroidal glycoalkaloids (SGAs) accumulate in red fruit of *GAME33*-overexpressing tomato plants. The cultivated (*S. tuberosum*) and wild (*S. chacoense*) potato *GAME33* genes (*StGAME33* and *ScGAME33*, respectively) were overexpressed in cultivated tomato (cv Micro Tom). (a–d) Levels of esculeoside A pathway SGAs (a, c) and prashantosi-*de* SGAs (b, d) are compared between red fruit of *StGAME33-Ox* (independent lines #2, #3 and #4), *ScGAME33-Ox* (independent lines #21 and #22) tomato plants and wild-type fruit. Overexpression of *GAME33* resulted in major accumulation of prashantosi-*de* SGAs with concomitant reduction in α -tomatine and other esculeoside A pathway intermediates in red fruit tissues. Values indicate means \pm SE ($n = 4$ for wild-type and $n = 3$ for individual transgenic lines genotype). Asterisks indicate significant changes compared to wild-type samples as calculated by a Student's *t*-test (*, $P < 0.05$; **, $P < 0.01$; ***, $P < 0.001$). LC-MS was used for targeted SGAs analysis.

these desaturated SGAs are not proper substrates for the enzymes acting downstream of α -tomatine or dehydrotomatine branch (e.g. GAME31 and GAME5; Fig. 1 for SGA pathway).

GAME40, a different 2-ODD enzyme, acts in the pathway downstream of α -tomatine towards esculeoside A formation

During the transition from the green to red fruit stage in tomato, the bitter α -tomatine is converted to esculeoside A, a nonbitter SGA (Sonawane *et al.*, 2018; Cárdenas *et al.*, 2019). This chemical shift involves four successive modifications of α -tomatine and formation of several pathway intermediates: hydroxytomatine (C-23 hydroxylation of α -tomatine), acetoxytomatine (O-acetylation of hydroxytomatine), acetoxy-hydroxytomatine (C-27 hydroxylation of acetoxytomatine) and esculeoside A (C-27 glucosylation of acetoxyhydroxytomatine) (Fig. 1). Recently, we have identified the GAME31 and GAME5 enzymes from tomato that catalyse the first C-23 hydroxylation (Cárdenas *et al.*, 2019) and last C-27 glucosylation of acetoxyhydroxytomatine (Szymanski *et al.*, 2020) steps in esculeoside A biosynthesis, respectively (Fig. 1, in green). As 2-ODD family members are largely involved in *Solanum* SGA modifications, we hypothesized that another 2-ODD-type enzyme could also carry out the C27-hydroxylation of acetoxytomatine to form acetoxy-hydroxytomatine.

In tomato, acetoxy-hydroxytomatine accumulates at breaker and red ripe stages of fruit ripening. First, we measured the levels of acetoxy-hydroxytomatine in 12 wild tomato accessions at the breaker and ripe stage. Acetoxy-hydroxytomatine (m/z 1108.55; $C_{52}H_{85}NO_{24}$) was detected in breaker and red fruit of all wild tomato accessions (Fig. 7a). Notably, very high levels of acetoxy-hydroxytomatine were observed in fruit of the *S. cheesmaniae* accession (#1306) as compared to fruit of other wild accessions. To discover the gene associated with acetoxy-hydroxytomatine biosynthesis, we explored the transcriptome data (generated in this study) for the candidate genes that are highly expressed in breaker and ripe stages of *S. cheesmaniae* accession (#1306). Notably, we discovered a 2-ODD candidate gene, which we termed here *GLYCOALKALOID METABOLISM40* (*GAME40*, Solyc09g089580) among the top 10 highly expressed genes in this *S. cheesmaniae* accession (#1306) (Dataset S2). Moreover, *GAME40* displayed a comparable expression profile in breaker and red fruit of other wild tomato accessions (Fig. 7b). The results suggested that *GAME40* is likely to be involved in hydroxylation of acetoxytomatine to acetoxy-hydroxytomatine.

Due to technical difficulties in purifying acetoxytomatine, the putative *GAME40* substrate, here we examined its enzyme activity in a coupled assay with additional upstream pathway enzymes. We expressed tomato *GAME40* in *E. coli* and performed an assay with two enzymes performing the two first steps from α -tomatine. These were the previously reported GAME31 and GAME36, an acyltransferase catalysing acetoxytomatine formation from hydroxytomatine (this will be published elsewhere; refer to Fig. 1 for esculeoside A pathway). Incubation of the three

enzymes with α -tomatine and the presence of acetyl-coA, α -ketoglutarate, ascorbate and Fe^{2+} yielded the expected product, acetoxy-hydroxytomatine (Fig. 7c). A positive control reaction containing the GAME31 enzyme and α -tomatine produced merely hydroxytomatine (23-hydroxytomatine). Interestingly, a reaction containing *GAME40* and α -tomatine also produced hydroxytomatine isomers but with different retention times than those produced by GAME31 (Fig. 7c). We predict that this newly formed hydroxytomatine isomer could be 27-hydroxytomatine, although detailed structural analysis is required to unambiguously confirm the structure. Acetoxy-hydroxytomatine was putatively identified by comparing retention times, elemental composition and fragmentation pattern with those described for the same in the literature (Itkin *et al.*, 2011; Iijima *et al.*, 2013; Schwahn *et al.*, 2014). An additional MS-MS analysis was performed to analyse the structures of enzyme assay products (Table S2).

Recently, Kazachkova *et al.* (2021) reported the discovery of the 'GORKY' glycoalkaloid transporter exporting α -tomatine and other SGAs from the vacuole to the cytosol. Several bitter flavour tomato accessions contain a deletion in *GORKY* that results in accumulation of the bitter α -tomatine and its downstream derivatives (e.g. hydroxytomatine and acetoxytomatine). Interestingly, one of the 'bitter' accessions (i.e. EA05978) accumulated high levels of α -tomatine, hydroxytomatine and acetoxytomatine as reported for other bitter accessions. Yet, EA05978 did not show any detectable levels of acetoxy-hydroxytomatine (the predicted *GAME40* reaction product) and esculeoside A (Kazachkova *et al.*, 2021). Next, we analysed the *GAME40* expression in ripe fruits of the Micro Tom (MT), 'Sweet cherry' and EA05978 cultivars. *GAME40* expression was not detected in the EA05978 accession as compared to the MT and Sweet cherry genotypes (Fig. 7d) that show normal accumulation of acetoxy-hydroxytomatine and esculeoside A in red fruit. Thus, in addition to a deletion in *GORKY*, the accession no. EA05978 contains a nonfunctional *GAME40* (likely a deletion in its genomic region), which prevents accumulation of acetoxy-hydroxytomatine and further esculeoside A in this accession.

Generating the diversity of tomato steroidal glycoalkaloids by combined expression of 2-ODD *GAME* genes *in planta*

We first examined the capacity of the cultivated tomato *GAME33* (*SIGAME33*, cloned from cv Micro Tom) to produce prashantoside SGAs *in planta* by infiltrating *N. benthamiana* leaves with *Agrobacterium* harbouring *SIGAME33* and α -tomatine as a substrate (infiltrated 3 d postagroinfiltration). The cultivated potato *GAME33* served as a positive control in these experiments as we demonstrated its activity in transgenic tomato (see previous section). We detected *de novo* production of prashantoside A and prashantoside B in the case of leaves infiltrated with either *SIGAME33* or *StGAME33* (Fig. S26a). In similar experiments, we examined the diverse activities of the various 2-ODD *GAME* genes acting at different positions on α -tomatine. We transiently co-expressed the tomato *GAME31*, *GAME33* and *GAME34* in *N. benthamiana* leaves (supplemented

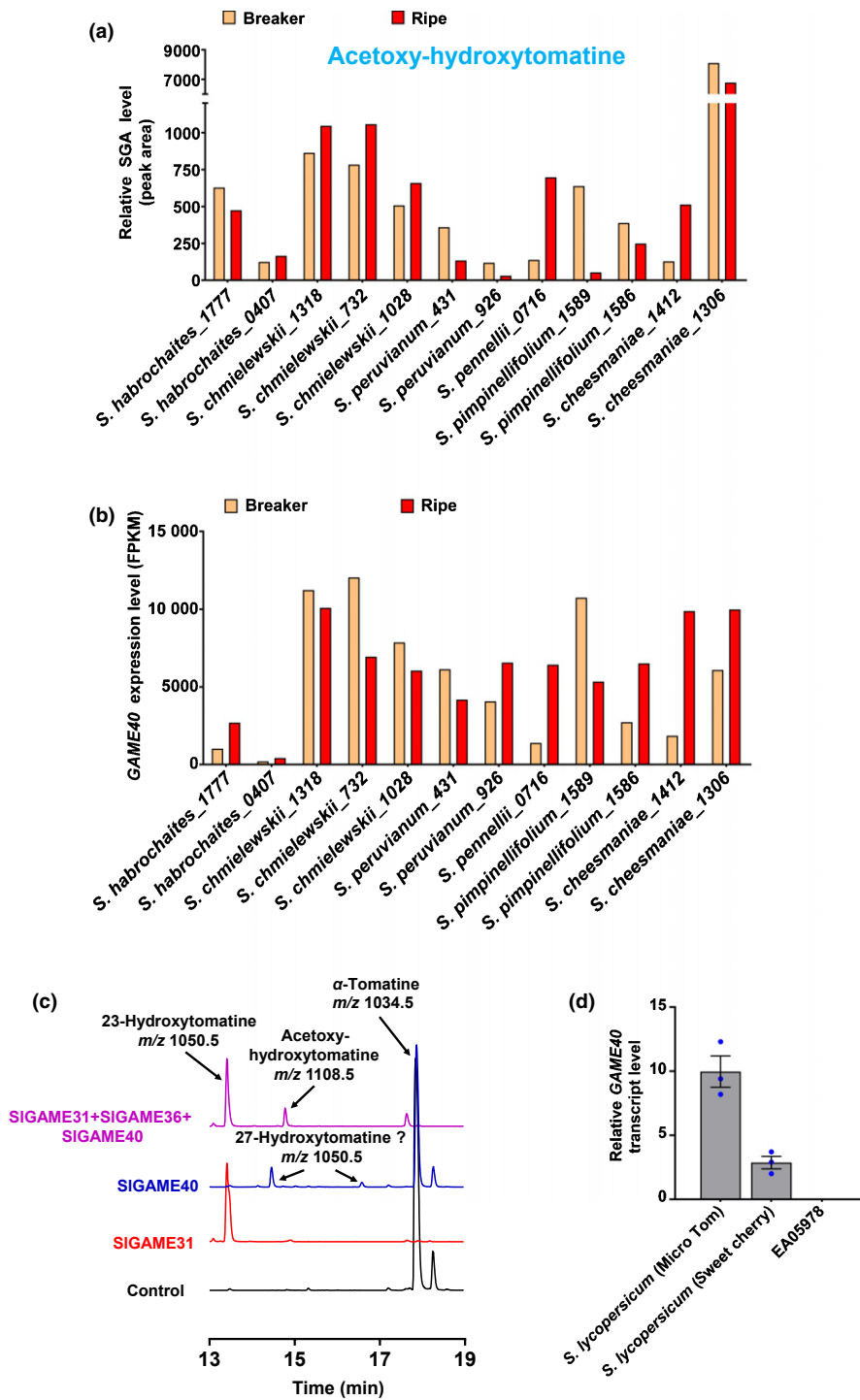


Fig. 7 Tomato GAME40 hydroxylates acetoxytomatine to acetoxy-hydroxytomatine in the biosynthetic pathway generating the nonbitter esculeoside A. (a) Levels of acetoxy-hydroxytomatine measured by LC-MS in different wild tomato species during breaker and ripe fruit stages of development ($n = 1$, single replicate for each fruit developmental stage was prepared by extracting several fruit from individual wild tomato species). SGA, steroidal glycoalkaloid. (b) Normalized GAME40 expression levels in breaker and ripe fruit developmental stages of wild tomato accessions. FPKM, fragments per kilobase of transcript per million mapped reads. (c) Recombinant SIGAME40, SIGAME31 and SIGAME36 enzymes (produced separately in *Escherichia coli* cells) convert α -tomatine to acetoxy-hydroxytomatine (in pink). Individual assays of GAME31 (in red) and SIGAME40 (in blue) recombinant enzymes convert α -tomatine to 23-hydroxytomatine and more likely to 27-hydroxytomatine, respectively. The control reaction (in black) contained α -tomatine substrate and the protein extracts of empty vector-transformed *E. coli* cells. Mass to charge (m/z) is shown for assay products. Enzyme assays analysis was carried out by LC-MS. (d) GAME40 gene expression in ripe fruit of cultivated tomato (cv Micro Tom and cv Sweet cherry) and bitter tomato accession (EA05978) as determined by qRT-PCR. The values shown in the bar graph indicate means of three biological replicates \pm SE ($n = 3$). GAME40 expression was not detected in the EA05978 tomato accession.

with α -tomatine) and detected the formation of all three corresponding SGAs products including hydroxytomatine, prashantoxide A and habrochaitoside A, respectively (Fig. S26b).

Discussion

Solanum SGAs are remarkable in structural diversity due to the enormous chemical modifications on their core scaffolds (Itkin *et al.*, 2011, 2013; Sonawane *et al.*, 2018; Cárdenas *et al.*, 2019).

Yet, despite the fundamental interest in this class of specialized metabolites, as well as their nutritional and medicinal properties, the biosynthetic pathways and related genes and enzymes are not entirely elucidated. In *Solanum* SGA biosynthesis, three cytochrome P450s activities (i.e. CYPs; GAME6, GAME8 and GAME4) reported so far are involved in generating the core scaffold (i.e. dehydrotomatidine) (Itkin *et al.*, 2013). However, as found in other pathways of specialized metabolism, members of the 2-ODD family could often carry out reactions typically

performed by CYP enzymes. To date, three 2-ODD enzymes (e.g. GAME11, GAME31 and GAME32) have been shown to act in the *Solanum* SGA pathway, performing different hydroxylation reactions (Fig. S1). Our work here further underscores the dominance of 2-ODDs activities over CYPs in SGA modifications as we discovered three new 2-ODD family enzymes in *Solanum* species (i.e. GAME33, GAME34 and GAME40). Our *in vivo* and *in vitro* results showed that the formation of habrochaitoside A and B from α -tomatine and dehydrotomatine, respectively, in wild tomato *S. habrochaites* is carried out by GAME34, and not by CYP450 as suggested earlier (Iijima *et al.*, 2013). In the past, the proposed biosynthetic pathway of habrochaitoside A suggested first, hydroxylation of α -tomatine to 20-hydroxytomatine, and further spontaneous reactions such as protonation, dehydration and rearrangement to form habrochaitoside A (Iijima *et al.*, 2013; Schwahn *et al.*, 2014). Recombinant GAME34 assays with α -tomatine did not generate a product resembling 20-hydroxytomatine but merely the final product habrochaitoside A. It might be possible that 20-hydroxytomatine is indeed formed as an intermediate metabolite in the enzyme assay reaction and utilized rapidly for successive spontaneous reactions to form habrochaitoside A. In fact, the LC-MS chromatogram of *GAME34-Ox* transgenic tomato leaves shows new peaks with m/z 1050.5 (corresponding to hydroxytomatine isomers) that have different retention times than normally found hydroxytomatine (23-hydroxytomatine). These peaks are difficult to isolate for further NMR studies as they are present in trace amounts and could be the 20-hydroxytomatine intermediate. Thus, the discovery of GAME34 enzyme activity in this study cannot confirm 20-hydroxytomatine as an intermediate in the biosynthesis of habrochaitoside A. The noteworthy anti-fungal activity demonstrated in this study by *GAME34-Ox* leaf extracts suggested the potential use of habrochaitoside A and derivatives as 'biocontrol agents' in crop protection against pathogens and predators. Nonetheless, overexpression of *GAME34* could be a valuable strategy to develop pathogen resistant *Solanum* plants by genetic engineering tools.

Akiyama *et al.* (2021) recently showed that DPS enzyme (identical to StGAME32-like) is involved in conversion of spirostanes to solanidanes in potato. Although orthologs of DPS enzymes were identified from nonsolanidane producing species, tomato (SlGAME33) and eggplant (SmGAME33), the corresponding *GAME33* genes are not expressed in these species. This suggests the loss of *GAME33* expression but significantly with no loss of function/activity (as demonstrated in this study), in nonsolanidane plants such as tomato and eggplant during evolution. Characterization of *GAME33* activity in the nonsolanidane producing *Solanum* species can be an example highlighting 'silent metabolism'. Silent metabolism defines metabolic capacities present in hidden or unused forms in plants that readily become functional when challenged (Lewinsohn & Gijzen, 2009; Kreis & Munkert, 2019). Silent metabolism provides an advantage to plants as it allows generating a large array of phytochemical diversity for survival and adaptation under challenging conditions. Several examples supporting silent metabolism in the terpenoid, carotenoid, volatile and phenylpropanoid biosynthetic pathways

have been described in various plant species (Lewinsohn & Gijzen, 2009). GAME33, a 2-ODD family member, is such an example of an enzyme that is expressed to very low levels in cultivated and wild tomato accessions, and does not possess any clear function under normal conditions. Conversely, *in vitro* assays with recombinant GAME33 enzyme (from several *Solanum* species) demonstrated its ability to produce prashantoside SGAs using core SAs and SGAs (via a desaturation reaction). When overexpressed in cultivated tomato, prashantoside A and B SGAs accumulated at the expense of core SGAs (i.e. α -tomatine and dehydrotomatine). Notably, prashantoside A and B SGAs have not been found in any *Solanum* species up to date. Yet, we could not rule out the possibility of their activity in very specialized tissues or cell types and under particular biotic or abiotic conditions.

Moreover, in this study, we identified another 2-ODD enzyme (i.e. GAME40) that acts in the pathway of esculeoside A and related ripening-associated SGAs. The functional diversity (in terms of hydroxylation capacity) displayed by GAME40 enzyme is also reflected in the phylogenetic analysis. GAME40 and its closest homolog GAME40-like (75% identity at amino acid level) from tomato appear in a completely different subclade (clade VI, dark red in Fig. 4) than rest of the 2-ODD GAME proteins acting in the SGA pathway (Fig. 4). Moreover, 13 2-ODD members (Fig. 4, 2-ODD-101 to 2-ODD-113) that are likely involved in ethylene biosynthesis are localized next to GAME40 subclade. This indicates functional diversification for GAME40 proteins in SGA metabolism over other related 2-ODD clade members involved in ethylene biosynthesis. Ethylene plays major role in tomato fruit ripening (Lincoln *et al.*, 1987; Lincoln & Fischer, 1988). The ripening-associated chemical shift in SGA metabolism (α -tomatine to esculeoside A) is also coordinated by ethylene-associated regulatory mechanisms. Higher levels of esculeoside A with low levels of α -tomatine were observed in wild-type tomato fruits treated with ethylene, while the ripening-impaired mutants *ripening-inhibitor* (*rin*), *non-ripening* (*nor*) and *never-ripe* (*Nr*) accumulated α -tomatine but showed reduced levels of esculeoside A compared to wild-type fruit (Iijima *et al.*, 2009). These results suggest that the late steps in the esculeoside A pathway depends on ethylene during ripening. GAME40 catalyses the penultimate step in the esculeoside A pathway by converting acetoxytomatine to acetoxyhydroxytomatine. In fact, the *GAME40* gene sequence reported here is identical to the *E8*, a known ethylene responsive gene crucial in tomato fruit ripening (Lincoln *et al.*, 1987; Lincoln & Fischer, 1988; Kneissl & Deikman, 1996). The *GAME40/E8* gene is known to be regulated by ethylene and several other transcription factors involved in fruit ripening (Fujisawa *et al.*, 2013). Tieman *et al.* (2017) showed that loss of *E8* function (by antisense silencing) modulated volatile biosynthesis in tomato. The authors suggested the role of *E8* in volatile biosynthesis although the precise action of *E8* remains unknown. In another study, Alonge *et al.* (2020) reported haplotype V (PI129033, *S. lycopersicum* var *cerasiforme*) that lacks *E8* due to a large 23-kbp deletion. In our study, we also reported one of the 'bitter' accessions (i.e. EA05978) that contains a nonfunctional GAME40 (Fig. 7d).

This accession accumulated high levels of α -tomatine, hydroxytomatine and acetoxytomatine but not any detectable levels of acetoxy-hydroxytomatine and esculeoside A (Kazachkova *et al.*, 2021). GAME40 activity shown here in the esculeoside A biosynthetic pathway links chemical shift in SGA metabolism with ethylene-associated tomato fruit ripening. Nevertheless, we cannot rule out the possibility of other functions of E8 in tomato fruit ripening. The formation of less toxic and nonbitter SGAs, like esculeoside A in ripe tomato fruit, from the toxic and bitter α -tomatine is important from an ecological point of view for promoting seed dispersal by frugivores.

Our findings demonstrate extensive involvement of 2-ODDs type enzymes in forming SGAs diversity suggests that this relatively little-explored protein family is key in unlocking the biosynthesis of numerous structures in the genus *Solanum* and moreover in SGAs-producing monocot species.




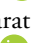


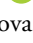
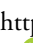


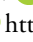
Acknowledgements


AA is the incumbent of the Peter J. Cohn Professorial Chair. We thank the Adelis Foundation, Leona M. and Harry B. Helmsley Charitable Trust, Jeanne and Joseph Nissim Foundation for Life Sciences, Tom and Sondra Rykoff Family Foundation Research and the Raymond Burton Plant Genome Research Fund for supporting the AA laboratory activity. The authors declare no competing interests.


Author contributions

PDS designed and performed the research and wrote the article. AJ contributed to data analysis and manuscript preparation. SP, BA, RB and YK assisted with the generation of transgenic plants. SM and IR assisted with metabolomics data analysis and operated the LC-MS. TU assisted in the protein expression and purification. GW and MP assisted in maintaining transgenic plants and sample collections. TS performed and analysed NMR experiments. AS provided the wild tomato accessions for metabolic and transcriptomic analysis. AD-F analysed transcriptome data from wild tomato accessions. SAG assisted in GAME40 enzyme characterization. APG assisted in data analysis. OR performed bioactivity assay against various pathogens. AA designed the research and wrote the article.

ORCID

Bekele Abebie  <https://orcid.org/0000-0003-3266-5122>
 Asaph Aharoni  <https://orcid.org/0000-0002-6077-1590>
 Ranjit Barbole  <https://orcid.org/0000-0001-5265-512X>
 Sachin A. Gharat  <https://orcid.org/0000-0002-2888-6371>
 Ashok P. Giri  <https://orcid.org/0000-0002-5309-259X>
 Adam Jozwiak  <https://orcid.org/0000-0002-7666-7747>
 Yana Kazachkova  <https://orcid.org/0000-0003-3613-4177>
 Sagit Meir  <https://orcid.org/0000-0001-7102-3152>
 Sayantan Panda  <https://orcid.org/0000-0002-5758-4700>
 Ilana Rogachev  <https://orcid.org/0000-0003-4452-2145>
 Tali Scherf  <https://orcid.org/0000-0002-2206-9426>

Prashant D. Sonawane  <https://orcid.org/0000-0002-3631-1703>

Tamar Unger  <https://orcid.org/0000-0002-6418-7949>

Guy Wizler  <https://orcid.org/0000-0002-4944-357X>

Data availability

Data supporting the findings of this work are available within the paper and its online Supporting Information files. RNA sequencing data generated from wild tomato accessions in the current study have been deposited into the NCBI with BioProject ID PRJNA798612.

References

- Akiyama R, Watanabe B, Nakayasu M, Lee HJ, Kato J, Umemoto N, Muranaka T, Saito K, Sugimoto Y, Mizutani M. 2021. The biosynthetic pathway of potato solanidanes diverged from that of spirosolanes due to evolution of a dioxygenase. *Nature Communications* 12: 1300.
- Along M, Wang X, Benoit M, Soyk S, Pereira L, Zhang L, Suresh H, Ramkrishnan S, Maumus F, Ciren D *et al.* 2020. Major impacts of widespread structural variation on gene expression and crop improvement in tomato. *Cell* 182: 145–161.
- Alseekh S, Tohge T, Wendenberg R, Scossa F, Omranian N, Li J, Kleessen S, Giavalisco P, Pleban T, Mueller-Roeber B *et al.* 2015. Identification and mode of inheritance of quantitative trait loci for secondary metabolite abundance in tomato. *Plant Cell* 27: 485–512.
- Cárdenas PD, Sonawane PD, Heinig U, Bocobza SE, Burdman S, Aharoni A. 2015. The bitter side of the nightshades: genomics drives discovery in Solanaceae steroidal alkaloid metabolism. *Phytochemistry* 113: 24–32.
- Cárdenas PD, Sonawane PD, Pollier J, Vanden Bossche R, Dewangan V, Weithorn E, Tal L, Meir S, Rogachev I, Malitsky S *et al.* 2016. GAME9 regulates the biosynthesis of steroidal alkaloids and upstream isoprenoids in the plant mevalonate pathway. *Nature Communications* 7: 10654.
- Cárdenas PD, Sonawane PD, Heinig U, Jozwiak A, Panda S, Abebie B, Kazachkova Y, Pliner M, Unger T, Wolf D *et al.* 2019. Pathways to defense metabolites and evading fruit bitterness in genus *Solanum* evolved through 2-oxoglutarate-dependent dioxygenases. *Nature Communications* 10: 5169.
- Chitwood DH, Kumar R, Headland LR, Ranjan A, Covington MF, Ichihashi Y, Fulop D, Jimenez-Gomez JM, Peng J, Maloof JN *et al.* 2013. A quantitative genetic basis for leaf morphology in a set of precisely defined tomato introgression lines. *Plant Cell* 25: 2465–2481.
- Eich E. 2008. *Solanaceae and convolvulaceae-secondary metabolites: biosynthesis chemotaxonomy biological and economic significance (a handbook)*. Berlin, Germany: Springer.
- Eshed Y, Zamir D. 1995. An introgression line population of *Lycopersicon pennellii* in the cultivated tomato enables the identification and fine mapping of yield-associated QTL. *Genetics* 141: 1147–1162.
- Farrow SC, Facchini P. 2014. Functional diversity of 2-oxoglutarate/Fe(II)-dependent dioxygenases in plant metabolism. *Frontiers in Plant Science* 5: 524.
- Friedman M. 2002. Tomato glycoalkaloids: role in the plant and in the diet. *Journal of Agriculture and Food Chemistry* 50: 5751–5780.
- Friedman M. 2006. Potato glycoalkaloids and metabolites: roles in the plant and in the diet. *Journal of Agriculture and Food Chemistry* 54: 8655–8681.
- Fujisawa M, Nakano T, Shima Y, Ito Y. 2013. A large-scale identification of direct targets of the tomato MADS box transcription factor RIPENING INHIBITOR reveals the regulation of fruit ripening. *Plant Cell* 25: 371–386.
- Hagel JM, Facchini PJ. 2018. Expanding the roles for 2-oxoglutarate-dependent oxygenases in plant metabolism. *Natural Product Reports* 35: 721.
- Iijima Y, Fujiwara Y, Tokita T, Ikeda T, Nohara T, Aoki K, Shibata D. 2009. Involvement of ethylene in the accumulation of esculeoside A during fruit ripening of tomato (*Solanum lycopersicum*). *Journal of Agriculture and Food Chemistry* 57: 3247–3252.

- Iijima Y, Watanabe B, Sasaki R, Takenaka M, Ono H, Sakurai N, Umemoto N, Suzuki H, Shibata D, Aoki K. 2013. Steroidal glycoalkaloid profiling and structures of glycoalkaloids in wild tomato fruit. *Phytochemistry* 95: 145–157.
- Islam MS, Lessing T, Chowdhury R, Hopkinson R, Schofield C. 2018. 2-oxoglutarate-dependent oxygenases. *Annual Review of Biochemistry* 87: 585–620.
- Itkin M, Heinig U, Tzfadia O, Bhide AJ, Shinde B, Cardenas PD, Bocobza SE, Unger T, Malitsky S, Finkers R *et al.* 2013. Biosynthesis of antinutritional alkaloids in Solanaceous crops is mediated by clustered genes. *Science* 341: 175–179.
- Itkin M, Rogachev I, Alkan N, Rosenberg T, Malitsky S, Masini L, Meir S, Iijima Y, Aoki K, de Vos R *et al.* 2011. GLYCOALKALOID METABOLISM1 is required for steroidal alkaloid glycosylation and prevention of phytotoxicity in tomato. *Plant Cell* 23: 4507–4525.
- Itkin M, Seybold H, Breitel D, Rogachev I, Meir S, Aharoni A. 2009. TOMATO AGAMOUS-LIKE 1 is a component of the fruit ripening regulatory network. *The Plant Journal* 60: 1081–1095.
- Jozwiak A, Sonawane PD, Panda S, Garagounis C, Papadopoulou KK, Abebie B, Massalha H, Almekias-Siegl E, Scherf T, Aharoni A. 2020. Plant terpenoid metabolism co-opts a component of the cell wall biosynthesis machinery. *Nature Chemical Biology* 16: 740–748.
- Kawai Y, Ono E, Mizutani M. 2014. Evolution and diversity of the 2-oxoglutarate-dependent dioxygenase superfamily in plants. *The Plant Journal* 78: 328–343.
- Kazachkova Y, Zemach I, Panda S, Bocobza S, Vainer A, Rogachev I, Dong Y, Ben-Dor S, Veres D, Kanstrup C *et al.* 2021. The GORKY glycoalkaloid transporter is indispensable for preventing tomato bitterness. *Nature Plants* 7: 468–480.
- Kneissl M, Deikman J. 1996. The tomato *E8* gene influences ethylene biosynthesis in fruit but not in flowers. *Plant Physiology* 112: 537–547.
- Kozukue N, Yoon K, Byun G, Misoo S, Levin C, Friedman M. 2008. Distribution of glycoalkaloids in potato tubers of 59 accessions of two wild and five cultivated *Solanum* species. *Journal of Agriculture and Food Chemistry* 56: 11920–11928.
- Kreis W, Munkert J. 2019. Exploiting enzyme promiscuity to shape plant specialized metabolism. *Journal of Experimental Botany* 70: 1435–1445.
- Lewinsohn L, Gijzen M. 2009. Phytochemical diversity: the sounds of silent metabolism. *Plant Science* 176: 161–169.
- Lincoln J, Cordes S, Read E, Fischer R. 1987. Regulation of gene expression by ethylene during *Lycopersicon esculentum* (tomato) fruit development. *Proceedings of the National Academy of Sciences, USA* 84: 2793–2797.
- Lincoln J, Fischer R. 1988. Diverse mechanisms for the regulation of ethylene-inducible gene expression. *Molecular and General Genetics* 212: 71–75.
- Mweetwa AM, Hunter D, Poe R, Harich KC, Ginzberg I, Veilleux RE, Tokuhisa JG. 2012. Steroidal glycoalkaloids in *Solanum chacoense*. *Phytochemistry* 75: 32–40.
- Nakayasu M, Umemoto N, Ohshima K, Fujimoto Y, Lee HJ, Watanabe B, Muranaka T, Saito K, Sugimoto Y, Mizutani M. 2017. A dioxygenase catalyzes steroid 16 α -hydroxylation in steroidal glycoalkaloid biosynthesis. *Plant Physiology* 175: 120–133.
- Ofner I, Lashbrooke J, Pleban T, Aharoni A, Zamir D. 2016. *Solanum pennellii* backcross inbred lines (BILs) link small genomic bins with tomato traits. *The Plant Journal* 87: 151–160.
- Sarrion-Perdigones A, Vazquez-Vilar M, Palaci J, Castelijn B, Forment J, Ziarolo P, Blanca J, Granell A, Orzaez D. 2013. GOLDENBRAID 2.0: a comprehensive DNA assembly framework for plant synthetic biology. *Plant Physiology* 162: 1618–1631.
- Schwahn K, Perez de Souza L, Fernie AR, Tohge T. 2014. Metabolomics-assisted refinement of the pathways of steroidal glycoalkaloid biosynthesis in the tomato clade. *Journal of Integrative Plant Biology* 56: 864–875.
- Sievers F, Wilm A, Dineen D, Gibson TJ, Karplus K, Li W, Lopez R, McWilliam H, Remmert M, Söding J *et al.* 2011. Fast scalable generation of high-quality protein multiple sequence alignments using Clustal Omega. *Molecular Systems Biology* 7: 539.
- Sonawane PD, Heinig U, Panda S, Gilboa NS, Yona M, Kumar SP, Alkan N, Unger T, Bocobza S, Pliner M *et al.* 2018. Short-chain dehydrogenase/reductase governs steroidal specialized metabolites structural diversity and toxicity in the genus *Solanum*. *Proceedings of the National Academy of Sciences, USA* 115: E5419–E5428.
- Sonawane PD, Jozwiak A, Panda S, Aharoni A. 2020. ‘Hijacking’ core metabolism: a new panache for the evolution of steroidal glycoalkaloids structural diversity. *Current Opinion in Plant Biology* 55: 118–128.
- Sonawane PD, Pollier J, Panda S, Szymanski J, Massalha H, Yona M, Unger T, Malitsky S, Arendt P, Pauwels L *et al.* 2016. Plant cholesterol biosynthetic pathway overlaps with phytosterols metabolism. *Nature Plants* 3: 16205.
- Szymański J, Bocobza S, Panda S, Sonawane P, Cárdenas PD, Lashbrooke J, Kamble A, Shahaf N, Meir S, Bovy A *et al.* 2020. Analysis of wild tomato introgression lines elucidates the genetic basis of transcriptome and metabolome variation underlying fruit traits and pathogen response. *Nature Genetics* 52: 1111–1121.
- Tamura K, Stecher G, Peterson D, Filipiński A, Kumar S. 2013. MEGA6: molecular evolutionary genetics analysis version 6.0. *Molecular Biology and Evolution* 30: 2725–2729.
- Tiemann D, Zhu G, Resende MFR, Lin T, Nguyen C, Bies D, Rambla JL, Beltran KSO, Taylor M, Zhang BO *et al.* 2017. A chemical genetic roadmap to improved tomato flavor. *Science* 355: 391–394.

Supporting Information

Additional Supporting Information may be found online in the Supporting Information section at the end of the article.

Dataset S1 GAME proteins and related homologues amino acid sequences used in the construction of phylogenetic tree.

Dataset S2 List of top 500 genes that are highly expressed in breaker stage of *S. cheesmaniae* accession #1306.

Fig. S1 Hydroxylation of diverse steroidal alkaloid substrates catalysed by three previously reported 2-ODDs, (i.e. GAME11, GAME31 and GAME32) in cultivated (tomato, Sl; eggplant, Sm) and wild (*Solanum chacoense*, Sc) *Solanum* species.

Fig. S2 Habrochaitoside B level in wild tomato accessions during four stages of fruit development.

Fig. S3 MS-MS analysis of habrochaitoside B.

Fig. S4 Ripening-associated SGAs profiling in two *Solanum habrochaites* accessions (#1777 and #0407).

Fig. S5 LC-MS-based SGAs analysis in two *Solanum habrochaites* accessions (#1777 and #0407) in mature green and ripe fruits.

Fig. S6 Profiling of habrochaitoside A in cultivated tomato and *GAME34/GAME35* candidate gene expression in tomato transcriptome.

Fig. S7 Habrochaitosides levels and *GAME34* candidate gene expression in tomato introgression lines.

Fig. S8 *GAME34* expression levels in different tissues of cultivated tomato (*Solanum lycopersicum* cv Micro Tom) at three developmental stages, as determined by quantitative real-time PCR (qRT-PCR).

Fig. S9 Aligned extracted ion chromatograms for habrochaitoside A and B comparison, and LC-MS analysis of recombinant GAME34 enzyme assay with tomatidine.

Fig. S10 Virus-induced gene silencing (VIGS) of *GAME34* in IL1-1 tomato line results in a major decrease in habrochaitoside A and B levels.

Fig. S11 Overexpression of *Solanum habrochaites* *GAME34* (*ShGAME34*) in cultivated tomato (cv Micro Tom) leads to ectopic accumulation of habrochaitoside A.

Fig. S12 Spore germination of *Puccinia* spp. fungi was completely inhibited by *GAME34*-Ox plant extracts.

Fig. S13 *GAME33* candidate gene expression.

Fig. S14 MS³ mass spectrum (1032.55→414.34) of Prashantoxide A, Habrochaitoside A and Dehydrotomatine.

Fig. S15 MS-MS analysis of Prashantoxide A-E (*GAME33*/*GAME32*-like enzyme assay products).

Fig. S16 LC-MS analysis of recombinant eggplant *GAME33* (*SmGAME33*) enzyme assay performed with SGA substrates.

Fig. S17 Characterization of the recombinant potato *GAME33* (*StGAME33*) by *in vitro* enzyme assays.

Fig. S18 Recombinant enzyme assays with *GAME33* from *Solanum chacoense* accession #8380-1.

Fig. S19 LC-MS analysis of recombinant potato *GAME32*-like (termed *StGAME32*-like) enzyme assay with SAs and SGAs substrates.

Fig. S20 *GAME33* expression in leaves, green and red ripe fruit of *GAME33*-overexpression transgenic tomato lines (quantitative real-time PCR assay).

Fig. S21 Overexpression of the *Solanum chacoense* *GAME33* (*ScGAME33*) and potato *GAME33* (*StGAME33*) in cultivated tomato leads to accumulation of newly formed prashantoxide SGAs in leaf tissues.

Fig. S22 Aligned total ion chromatograms showing *de novo* accumulation of prashantoxide SGAs in leaves of *ScGAME33*-overexpressing (*ScGAME33*-Ox) and *StGAME33*-overexpressing (*StGAME33*-Ox) transgenic tomato lines.

Fig. S23 Overexpression of *GAME33* alters SGAs composition in green fruit.

Fig. S24 Comparisons of SGA profiles of wild-type, *StGAME33*- and *ScGAME33*-overexpressing transgenic tomato lines.

Fig. S25 Levels of esculeoside A isomers and derivatives in *GAME33*-overexpressed tomato red fruits.

Fig. S26 Transient expression of several 2-ODD *GAME* genes in *Nicotiana benthamiana* produces diverse steroidal glycoalkaloids derivatives.

Methods S1 LC-MS based SGA analysis, *E. coli* expression and *in vitro* assays for *GAME* enzymes, Transient expression in *N. benthamiana* and tomato (cv VF36), *GAME34*-VIGS in IL1-1 tomato plants, Habrochaitoside A purification for NMR analysis, NMR spectroscopy, Microplate based analysis of *GAME34*-Ox leaf extracts for germination inhibition of *Puccinia* spores.

Notes S1 HMBC correlations of the hydrogens atoms observed in habrochaitoside A NMR analysis.

Notes S2 ¹H NMR spectrum (600 MHz, MeOD-d₄) of habrochaitoside A.

Notes S3 ¹³C DEPTQ NMR spectrum (150 MHz, MeOD-d₄) of habrochaitoside A.

Notes S4 2D dqf-COSY NMR spectrum of habrochaitoside A.

Notes S5 2D ROESY NMR spectrum of habrochaitoside A.

Notes S6 2D HSQC NMR spectrum of habrochaitoside A.

Notes S7 2D HMBC NMR spectrum of habrochaitoside A.

Table S1 ¹H and ¹³C NMR spectroscopic data of habrochaitoside A, split into the aglycone (left) and sugar (right) parts of the molecule.

Table S2 MS-based identification of *GAME40* enzyme assay products.

Please note: Wiley Blackwell are not responsible for the content or functionality of any Supporting Information supplied by the authors. Any queries (other than missing material) should be directed to the *New Phytologist* Central Office.